

Report

**R-19-04**

January 2019



# Development of methodology for flow path analysis in the surface system – Numerical modelling in MIKE SHE for Laxemar

**A report for the safety evaluation SE-SFL**

**Emma Johansson**

**Mona Sassner**

SVENSK KÄRNBRÄNSLEHANTERING AB

SWEDISH NUCLEAR FUEL  
AND WASTE MANAGEMENT CO

Box 3091, SE-169 03 Solna  
Phone +46 8 459 84 00  
skb.se

SVENSK KÄRNBRÄNSLEHANTERING



ISSN 1402-3091

**SKB R-19-04**

ID 1615945

January 2019

# **Development of methodology for flow path analysis in the surface system – Numerical modelling in MIKE SHE for Laxemar**

**A report for the safety evaluation SE-SFL**

Emma Johansson

Svensk Kärnbränslehantering AB

Mona Sassner

DHI Sverige AB

A pdf version of this document can be downloaded from [www.skb.se](http://www.skb.se).

© 2019 Svensk Kärnbränslehantering AB



## Abstract

This study was performed within the framework of the safety evaluation for the planned repository for long lived waste (SFL). The hydrological flow pathways and travel times through different layers of Quaternary deposits have been in focus. The aim of the study was to develop a methodology for a detailed flow path analysis within different biosphere objects of the surface system, to be used when exporting hydrological fluxes from the MIKE SHE model to the dose model. The motivation for this study was the limitation in the numerical implementation of geological layers in previous versions of the MIKE SHE model, where the uppermost geological layers in the surface system have been lumped together in one numerical calculation layer. This limits the possibilities for a detailed flow path analysis in the surface systems. To investigate the effect of this simplification on the calculated flow pathways, this study is focused on updating the numerical implementation of the geological layers as a first step. In a second step, the new implementation was tested by performing particle tracking calculations through the defined biosphere objects in the area. The particle tracking results enabled a quantification of the groundwater flow paths and travel times through each layer of the Quaternary deposits underlying the biosphere objects. In the last step, the detailed flow paths analysis was used as input when defining the areas for which water balances of the biosphere objects are exported from MIKE SHE to the dose model. This results in a “flow path dependent” water balance, where only the areas within a biosphere object exposed to groundwater discharge are used when defining fluxes exported from MIKE SHE to the dose model. The model study was based and further elaborated on the Laxemar 2.3 model.

## Sammanfattning

Denna studie har genomförts inom ramen för säkerhetsvärderingen av det planerade slutförvaret för långlivat avfall, SFL. Grundvattnets flödesvägar och flödestider genom olika jordlager i ytekosystemen har varit fokus i studien. Syftet var att utveckla en metod för att bättre kunna beskriva flödesvägar inom olika biosfärsobjekt i ytsystemet, som sen ska komma att användas vid export av hydrologiska flöden från MIKE SHE modellen till dosmodellen. Bakgrunden till studien är de numeriska begränsningar som finns i implementeringen av geologiska lager i MIKE SHE. I tidigare versioner av MIKE SHE modellen har de översta geologiska lagren slagits ihop till ett tjockare numeriskt lager vilket har begränsat möjligheterna till en detaljerad beskrivning av flödesvägarna genom de översta jordlagren. För att undersöka effekten av dessa begränsningar fokuserar den här studien i ett första steg på att uppdatera den numeriska implementeringen av jordlagren. I nästa steg har den nya beskrivningen av jordlagren testats med hjälp av partikelspårning, där vattenpaket märks och spåras genom de olika jordlagren inom biosfärsobjekten. Resultaten från partikelspårningen gjorde det möjligt att kvantifiera såväl flödesvägar som flödestider genom varje enskilt jordlager som underlagrar biosfärsobjekten. I ett sista steg användes resultaten för att identifiera de områden för vilka vattenbalanser från MIKE SHE modellen till dosmodellen ska exporteras. Det resulterade i en vattenbalans som tar hänsyn till flödesvägarna för utströmmande grundvatten genom varje biosfärsobjekt så att det endast är de områden av varje objekt som faktiskt exponeras för utströmning av djupt grundvatten som används när flöden exporteras från MIKE SHE till dosmodellen. Den här studien baserades helt på den tidigare etablerade MIKE SHE modellen L2.3 för Laxemar.

# Contents

<b>1</b>	<b>Introduction</b>	7
1.1	Related modelling activities	8
<b>2</b>	<b>Material and methods</b>	9
2.1	Site description and hydrological conceptual model	9
2.2	Summary of input and calibration data	12
2.3	Numerical modelling methodology	14
2.3.1	Regional and local model area	14
2.3.2	Flow modelling	16
2.3.3	Transport modelling	19
<b>3</b>	<b>Results</b>	23
3.1	Sensitivity analysis of numerical implementation of geological soil layers	23
3.2	Transport modelling in local model	28
3.3	Converting information from Mike SHE to dose models	31
<b>4</b>	<b>Summary and discussion</b>	39
	<b>References</b>	41
<b>Appendix</b>	Tables with MAE and ME values	43



# 1 Introduction

The present work is part of the SFL safety evaluation, i.e the safety evaluation for the planned repository for long-lived low and intermediate level waste. In order to provide input to the site selection process for SFL the safety evaluation aims at evaluating the proposed repository concept (Elfving et al. 2013) at a representative site in Sweden. The evaluation will be performed with existing data from SKB's site investigation programs for the nuclear fuel repository in Laxemar and Forsmark. In the present work the hydrology and near surface hydrogeology of the Laxemar area, Figure 1-1, is studied.

The modelling reported in this document is focused on the flow paths of discharging groundwater from the bedrock into the surface systems and the transport of water in Quaternary deposits (QD) and surface water systems. The modelling was performed using the MIKE SHE tool (Graham and Butts 2005). The main objective of the modelling was to further develop the established method for deriving hydrological and hydrogeological fluxes appropriate for dose model calculations from MIKE SHE water balances (Bosson et al. 2010, Werner et al. 2013). The method development was divided into two main steps. First, an analysis of the numerical implementation of geological units and its influence on the water flow paths in the QD was performed. Based on the result from step one, a detailed analysis of the water flow path through the different geological units was performed with the aim to define "flow path dependent" water balances.

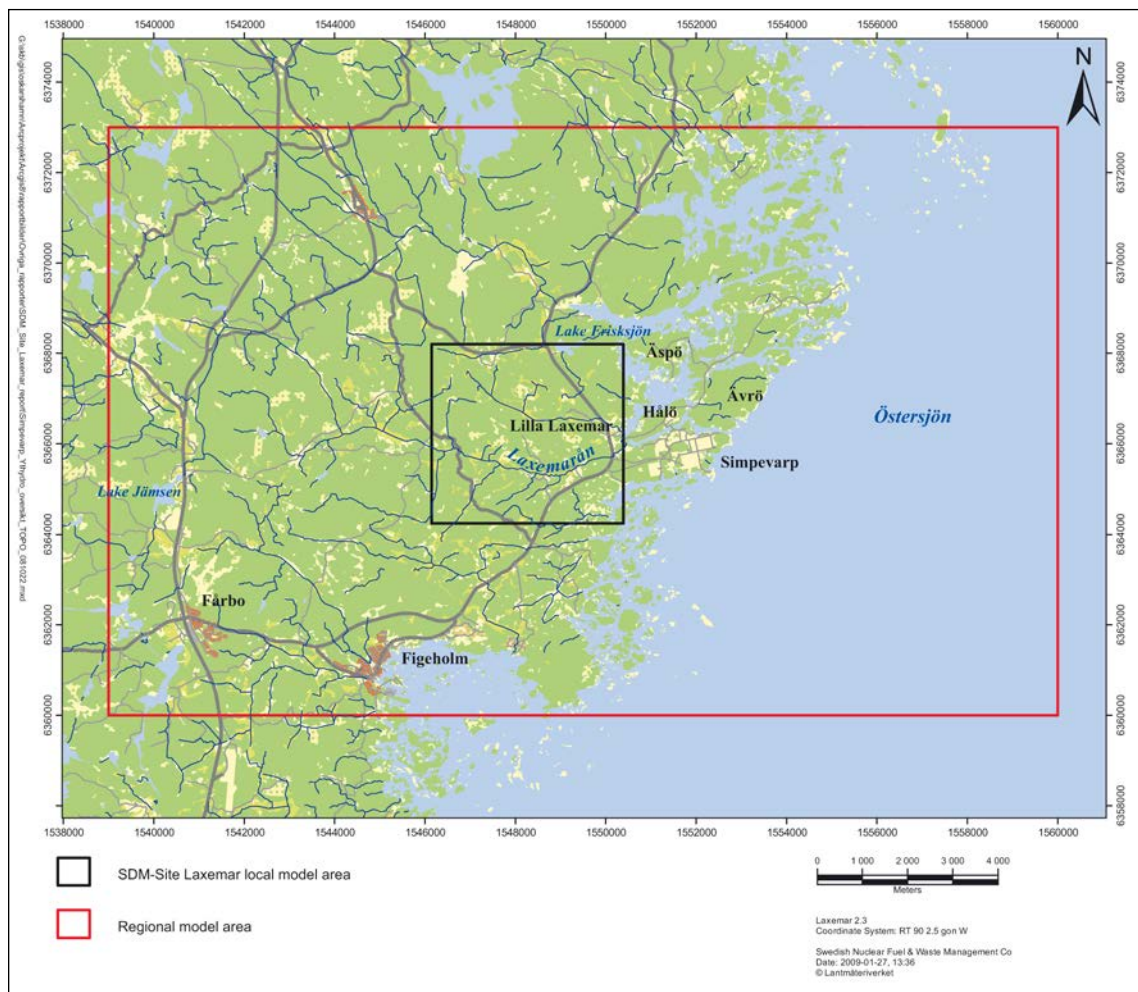


**Figure 1-1.** The local and regional model areas in Laxemar as defined in the Site descriptive modelling of the Laxemar area (Söderbäck and Lindborg 2009).

## 1.1 Related modelling activities

The present work is based on two other modelling activities which are listed below. The two models have provided input to the present MIKE SHE model.

**MIKE SHE SDM 2.3-model:** The MIKE SHE SDM 2.3 model reported in Bosson et al. (2009) was used as starting point in the present work. No model updates have been done in the present work except from the model area, the stream network which is numerically implemented in the modelling tool Mike11 (Bosson et al. 2009), and the numerical representation of geological layers in the QD. The changes are described in Section 2.2.

**Connectflow:** The hydrogeological modelling within the framework of SFL is performed in the modelling tool ConnectFlow reported in Joyce et al. (2019). Particle positions (case sfl\_elaborated\_r1\_hrd\_site\_nochem\_pline\_surfaces\_2000, Joyce et al. 2019) at the QD/bedrock interface was imported to the MIKE SHE model for further tracing in the surface systems, i.e. the QD layers and terrestrial and limnic ecosystems above the bedrock.

## 2 Material and methods

### 2.1 Site description and hydrological conceptual model

The topography of the Laxemar-Simpevarp area is characterised by relatively distinct valleys, surrounded by higher-altitude areas dominated by exposed rock or areas with very thin soil layers. The south-western and central parts of the Laxemar-Simpevarp area (Figure 1-1) are characterised by hummocky moraine and thereby by a smaller-scale topography. Almost the whole area is located below 50 m.a.s.l. and the entire area is located below the highest coastline. The Quaternary deposits in the area, Figure 2-1, are described in Sohlenius and Hedenström (2008).

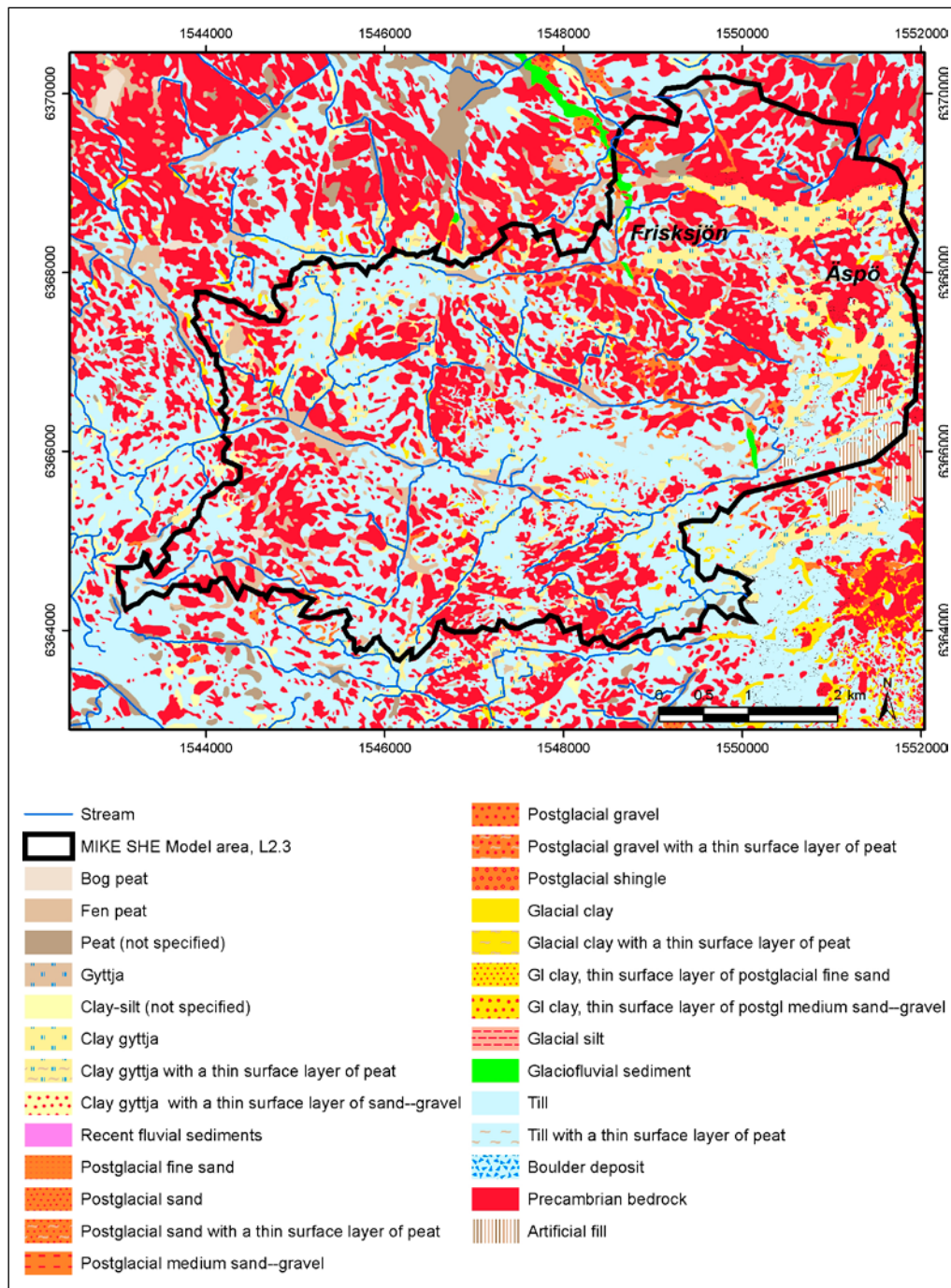
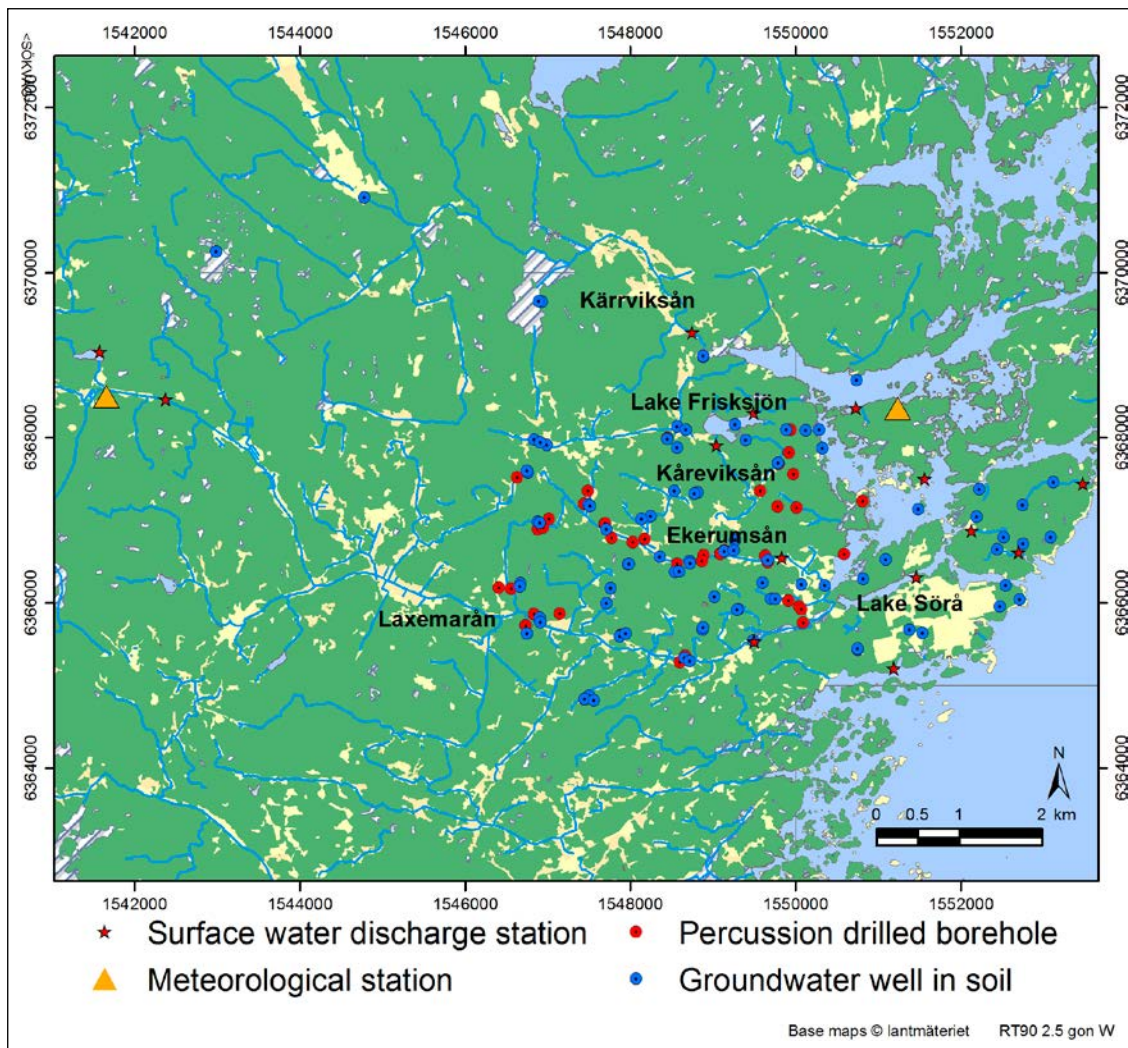


Figure 2-1. Map of Quaternary deposits in the Laxemar area.



**Figure 2-2.** Lakes, streams and monitoring points in the Laxemar area.

Six lakes are found within the Laxemar-Simpevarp area; Lake Jämsen (0.24 km<sup>2</sup>), Lake Frisksjön (0.13 km<sup>2</sup>), Lake Sörå (0.10 km<sup>2</sup>), Lake Plittorpsgöl (0.03 km<sup>2</sup>), Lake Fjällgöl (0.03 km<sup>2</sup>) and Lake Grangöl (no size data), see Figure 1-1 and 2-2. Only Lake Frisksjön and Lake Sörå are situated inside the MIKE SHE model area. The lakes are relatively small and shallow with mean depths ranging from 1–4 m. The streams are affected by land improvement and drainage operations due to agricultural activity. The largest streams Laxemarån, Kåreviksån, downstream from Lake Frisksjön, and Kärrviksån (Figure 2-2) are flowing throughout the year and the smaller streams are dry during approximately half of the year.

Within the framework of the site-descriptive modelling of the hydrology at Laxemar (Werner 2009), four main hydrogeological type areas were defined based on the type and depths of the Quaternary deposits: High-altitude areas, large and small valleys, glaciofluvial deposits, and hummocky moraine areas. The general characteristics of groundwater recharge and discharge patterns are described for each type area in Werner (2009).

In the QD, observations from the site investigations (2003–2007) show that groundwater levels are shallow and the depth to the groundwater table is on average less than one metre during 50 % of the time (Werner et al. 2008). In general, the depth to the groundwater table is larger in high-elevation areas compared to low-elevation areas and there is a close correlation between the ground-surface topography and groundwater levels in the QD. The groundwater table in the valleys and agricultural areas, which are in focus in the present study, are typically only a few decimetres below ground and the levels are transient during the year depending on weather conditions (Werner et al. 2008). The

recharge and discharge patterns of groundwater in the near surface system is hence influenced by the local topography. Figure 2-3 illustrates the overall conceptual model of hydrology and hydrogeology in Laxemar. The different type areas and a more detailed description of the conceptual understanding of the hydrology in Laxemar are given in Werner (2009) and hydrogeology and bedrock hydrogeology are described in Rhén et al. (2009).

Except for some minor wetlands, the surface waters (lakes, streams and wetlands) are associated with low-altitude areas. These surface waters are mainly underlain by glacial and post-glacial sediments. Specifically, the general bottom-up regolith stratigraphy below surface waters is till and glacial clay, overlain by postglacial sediments (sand/gravel, gyttja clay/clay gyttja, overlain by fen peat and bog peat in the wetlands).

The hydraulic conductivity of the rock generally decreases with depth, both in the deterministically described deformation zones and in the rock between these zones. The deformation zones are mostly sub-vertical, i.e. dipping, and typically one order of magnitude more conductive than the surrounding rock. Many deformation zones coincide with and outcrop in valleys. In the background rock between the deformation zones, there is a more pronounced decrease with depth of the intensity of sub-horizontal fractures compared to sub-vertical fractures. As can be seen in Figure 2-3, the deformation zones vary in thickness, and are generally wider closer to the interface between Quaternary deposits and bedrock.

From a conceptual point of view, the bedrock in Laxemar can hydrogeologically be divided and described in terms of the following depth intervals, here denoted dZ1–dZ4 (cf. Figure 2-3) (Werner 2009, Rhén et al. 2009):

- dZ1 (0–150 m): Near-surface rock, characterised by a high frequency of conductive fractures.
- dZ2 (150–400 m): Intermediate-depth rock, characterised by an intermediate frequency of conductive fractures.
- dZ3 (400–650 m): Rock at repository level, characterised by a low frequency of conductive fractures.
- dZ4 (650 m and deeper): Deep rock, characterised by a sparse network of conductive fractures.

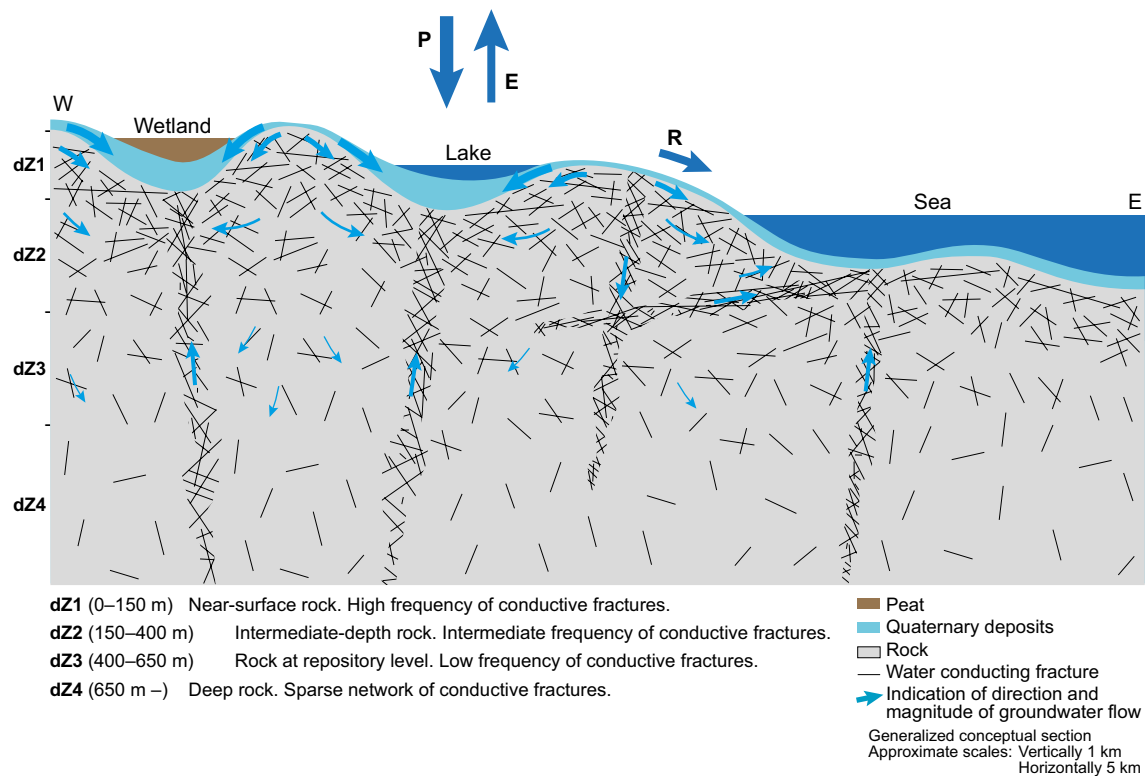


**Figure 2-3.** Conceptual model of hydrology and near surface hydrogeology in Laxemar (from Werner 2009). The light blue arrows indicate the dominating direction and magnitude of groundwater flow.

## 2.2 Summary of input and calibration data

The MIKE SHE model includes spatial data, describing the geometries, hydrological and hydrogeological properties of the bedrock and QD, the topography, and time series data for meteorological parameters. Time series of surface- and groundwater levels in bedrock and QD, together with time series data on surface water discharge, are used as calibration and validation data. In the present work the MIKE SHE model from the site descriptive modelling version 2.3 (SDM L2.3) is used as starting point. The modelling work included in the present work only contains changes to the numerical description of the different QD-layers, i.e. no changes are made to the input data compared to the reported SDM 2.3 MIKE SHE model. The model is described in detail in Bosson et al. (2009). Below follows a short description of the used input and calibration data.

The L2.3 model was calibrated to data for the period from October 10, 2003, to December 31, 2006, and the model was validated using data from between January 1, 2007, and December 31, 2007.

**Meteorology:** The MIKE SHE model uses data on temperature, precipitation and potential evapotranspiration. Locally measured data are available for the whole simulation period, i.e. between October 10, 2003, and December 31, 2007. The meteorological input data are taken from two meteorological stations, the Plittorp and Äspö stations (see Figure 2-2). A clear gradient with increasing precipitation from coast to inland has been identified (Werner et al. 2008) therefore the meteorological input data has been divided into three zones in the model, the western zone (based on data from the Plittorp station), the east zone (based on data from the Äspö station), and the middle zone (based on data from both stations). Details about the meteorological data are further described in Werner et al. (2008).

**Bedrock hydrogeology:** Input to the hydrogeological description of the bedrock is obtained from the ConnectFlow groundwater flow model (Rhén et al. 2009). The horizontal resolutions of the data describing the hydraulic properties of the bedrock are  $40 \times 40$  m, i.e. the same as the MIKE SHE model grid. The vertical resolution of the hydrogeological properties of the bedrock is also 40 m. Data representing the horizontal distribution of properties are introduced to the MIKE SHE model as geological layers every 40 m. The model is based on the L2.3 geological model.

**Quaternary deposits (QD):** The input data describing the QD in the MIKE SHE SDM-Site model, as described in Bosson et al. (2009) are based on three main inputs; the map of Quaternary deposits (Sohlenius and Hedenström 2008), the model of regolith depth and stratigraphy in Laxemar, Figure 2-4 and Table 2-1 (Nyman et al. 2008) and the dataset describing the hydraulic properties of the QD (Werner 2009). In the present work no changes have been made to the hydraulic properties assigned to the MIKE SHE model reported in Bosson et al. (2009), the properties are listed in Table 2-2 and Table 2-3.

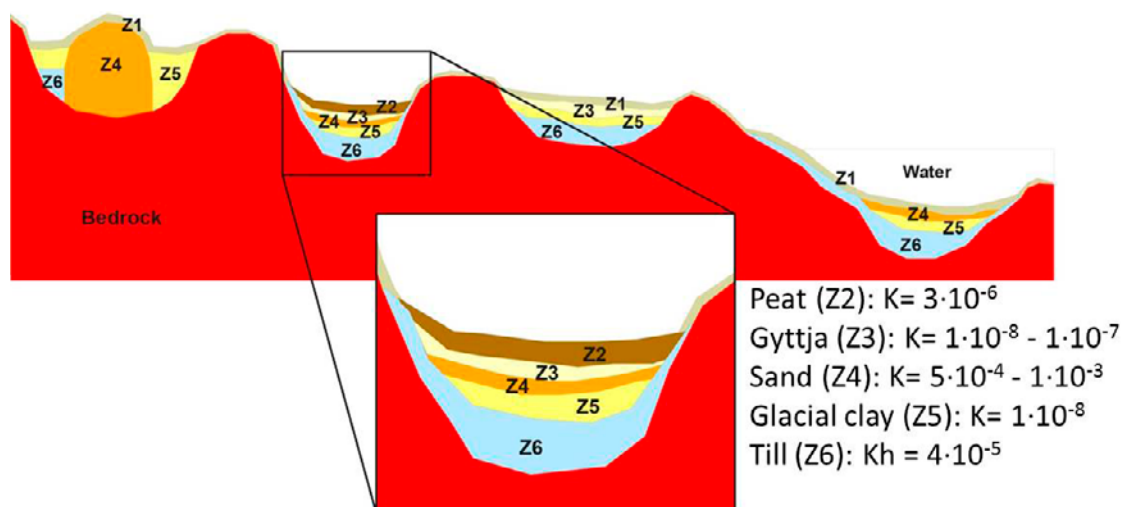


**Figure 2-4.** Upper figure: Conceptual model of the regolith depth model for Laxemar. The different Z-layers represent the different type of QD present in the Laxemar area. The uppermost layer Z1 represents several types of QD, see Table 2-1. Lower figure: Hydraulic conductivity values (m/s) for each Z-layer in a typical soil profile in an agricultural area.

The applied hydraulic conductivity values for wetland and agricultural areas, which are in focus for the transport modelling performed in the present work, are schematically described in the lower figure in Figure 2-4. The figure represents a profile through peat area which is underlain by gyttja, sand and clay.

**Table 2-1. Description of layers Z1 to Z6.**

Layer	Description
Z1	This layer represents the uppermost regolith and is present within the entire model area, except in areas covered by peat. On bedrock outcrops, the thickness of the layer is set to 0.1 m and in other areas to 0.6 m. If the regolith depth is less than 0.6 m, Z1 will be the only layer. In the terrestrial areas this layer is assumed to be affected by soil forming processes.
Z2	This layer is present where <b>peat</b> is shown on the map of Quaternary deposits (QD).
Z3	The layer represents <b>postglacial clay gyttja, gyttja or recent fluvial sediments</b> .
Z4	This layer represents <b>postglacial coarse-grained sediments (mostly sand and gravel), artificial fill and glaciofluvial material</b> . Z4 rests directly upon the bedrock surface in areas shown as glaciofluvial sediment or artificial fill on the QD map. Z4 is always underlain by glacial clay (Z5) and till (Z6) in areas where postglacial sand/gravel is shown on the QD map.
Z5	The layer represents <b>glacial clay</b> .
Z6	This layer represents <b>glacial till</b> , which is the most common QD in the model area. The thickness of Z6 is zero if the total QD depth is < 0.6 m (e.g. at bedrock outcrops) or if Z4 (see above) rests directly on the bedrock surface. The lower boundary of layer Z6 represents the bedrock surface, which means that the lower level of Z6 constitutes a DEM for the bedrock surface.

**Table 2-2. Hydraulic conductivities (m/s), Specific Yield (-) and Specific storage (1/m) for the QD-classes in layer Z1 (Figure 2-4).**

Z1	Kh [m/s]	Kv [m/s]	Sy [-]	Ss [1/m]
Bedrock	$4 \times 10^{-4}$	$4 \times 10^{-4}$	0.1	$5 \times 10^{-3}$
Till	$4 \times 10^{-4}$	$4 \times 10^{-4}$	0.15	$1 \times 10^{-3}$
Till with a thin surface layer of peat	$3 \times 10^{-6}$	$3 \times 10^{-6}$	0.24	$5 \times 10^{-2}$
Post glacial shingle	$1 \times 10^{-2}$	$1 \times 10^{-2}$	0.25	0.025
Boulder deposit	$4 \times 10^{-4}$	$4 \times 10^{-4}$	0.15	$1 \times 10^{-3}$
Gyttja clay/clay gyttja	$4 \times 10^{-4}$	$4 \times 10^{-4}$	0.1	$1 \times 10^{-3}$
Gyttja	$4 \times 10^{-4}$	$4 \times 10^{-4}$	0.1	$5 \times 10^{-3}$
Gyttja clay/clay gyttja with a thin surface layer of peat	$3 \times 10^{-6}$	$3 \times 10^{-6}$	0.24	$5 \times 10^{-2}$
Recent fluvial sediments	$4 \times 10^{-4}$	$4 \times 10^{-4}$	0.1	$5 \times 10^{-3}$
Gyttja clay/clay gyttja with a thin surface layer of sand/gravel	$5 \times 10^{-3}$	$5 \times 10^{-3}$	0.25	0.025
Peat	$3 \times 10^{-6}$	$3 \times 10^{-6}$	0.24	$5 \times 10^{-2}$
Glacial clay	$4 \times 10^{-4}$	$4 \times 10^{-4}$	0.1	$5 \times 10^{-3}$
Glacial clay with a thin surface layer of postglacial fine sand	$5 \times 10^{-4}$	$5 \times 10^{-4}$	0.25	0.025
Glacial clay with a thin surface layer of postglacial medium sand/gravel	$5 \times 10^{-3}$	$5 \times 10^{-3}$	0.25	0.025
Clay-silt	$4 \times 10^{-4}$	$4 \times 10^{-4}$	0.1	$5 \times 10^{-3}$
Postglacial fine sand	$4 \times 10^{-4}$	$4 \times 10^{-4}$	0.1	$5 \times 10^{-3}$
Postglacial sand	$4 \times 10^{-4}$	$4 \times 10^{-4}$	0.1	$5 \times 10^{-3}$
Postglacial sand with a thin layer of peat	$3 \times 10^{-6}$	$3 \times 10^{-6}$	0.24	$5 \times 10^{-2}$
Postglacial medium sand/gravel	$4 \times 10^{-4}$	$4 \times 10^{-4}$	0.1	$5 \times 10^{-3}$
Postglacial gravel with a thin surface layer of peat	$3 \times 10^{-6}$	$3 \times 10^{-6}$	0.24	$5 \times 10^{-2}$
Postglacial gravel	$4 \times 10^{-4}$	$4 \times 10^{-4}$	0.1	$5 \times 10^{-3}$
Glacial clay with a thin surface layer of peat	$3 \times 10^{-6}$	$3 \times 10^{-6}$	0.24	$5 \times 10^{-2}$
Glacial silt	$4 \times 10^{-4}$	$4 \times 10^{-4}$	0.1	$5 \times 10^{-3}$
Glaciofluvial sediments	$4 \times 10^{-4}$	$4 \times 10^{-4}$	0.1	$5 \times 10^{-3}$
Artificial fill	$4 \times 10^{-4}$	$4 \times 10^{-4}$	0.1	$5 \times 10^{-3}$

**Table 2-3. Hydraulic conductivities (m/s), Specific Yield (-) and Specific storage (1/m) for the QD-classes in layer Z2-Z6 (Figure 2-4).**

	Kh [m/s]	Kv [m/s]	Sy [-]	Ss [1/m]
<b>Z2</b>				
Peat	$3 \times 10^{-6}$	$3 \times 10^{-6}$	0.24	$5 \times 10^{-2}$
<b>Z3</b>				
Postglacial gyttja				
Gyttja	$1 \times 10^{-8}$	$1 \times 10^{-8}$	0.03	$6 \times 10^{-3}$
Recent fluvial sediments	$1 \times 10^{-7}$	$1 \times 10^{-7}$	0.03	$6 \times 10^{-3}$
Gyttja clay/Clay gyttja	$1 \times 10^{-7}$	$1 \times 10^{-7}$	0.03	$6 \times 10^{-3}$
<b>Z4</b>				
Post glacial fine sand	$5 \times 10^{-4}$	$5 \times 10^{-4}$	0.25	0.025
Post glacial sand	$1 \times 10^{-3}$	$1 \times 10^{-3}$	0.25	0.025
Post glacial medium sand-gravel	$5 \times 10^{-3}$	$5 \times 10^{-3}$	0.25	0.025
Post glacial gravel	$1 \times 10^{-2}$	$1 \times 10^{-2}$	0.25	0.025
Glacial silt	$5 \times 10^{-3}$	$5 \times 10^{-3}$	0.25	0.025
Glaciofluvial sediments	$5 \times 10^{-3}$	$5 \times 10^{-3}$	0.25	0.025
Artificial fill	$5 \times 10^{-5}$	$5 \times 10^{-5}$	0.05	$1 \times 10^{-3}$
<b>Z5</b>				
Glacial clay	$1 \times 10^{-8}$	$1 \times 10^{-8}$	0.25	0.025
<b>Z6</b>				
Glacial till	$4 \times 10^{-5}$	$4 \times 10^{-5}$	0.05	$1 \times 10^{-3}$

**Stream and lake data:** Data on lake thresholds and bathymetry levels, cross sections of the water courses and the extension of the river network have been used as input to the description of the surface water system. Cross sections of the streams have been measured along all major streams in the area (Strömngren et al. 2006). The stream network is implemented in the tool MIKE11 which runs together with the MIKE SHE model and water is exchanged between the ground surface, the groundwater and the river network throughout the simulation (Bosson et al. 2009).

**Calibration data:** In the present work, no thorough calibration of the model properties was made. Since the model changes only relates to the numerical grid and description of the different QD-layers a comparison of calculated ground- and surface water levels and surface water discharges from the SDM-model and the present model were made. However, for comparison of model results between the MIKE SHE SDM model and the present model the same observation points were used as during the MIKE SHE SDM-model calibration. This includes data from one surface water level monitoring station, four surface water discharge monitoring stations, 33 groundwater monitoring wells in Quaternary deposits, and 39 observation points (sections) in percussion-drilled boreholes in bedrock (Figure 2-2).

## 2.3 Numerical modelling methodology

### 2.3.1 Regional and local model area

Two model areas were defined, one regional area for the flow modelling and one local area for transport modelling applications. The regional model area has a horizontal grid resolution of  $40 \times 40$  m and the local model  $10 \times 10$  m. The vertical discretization of the SDM2.3 model was used as a starting point in the regional flow modelling. The influence of the numerical description of the QD-layers on the groundwater flow paths was analysed in detail and is further described in Section 2.3.2.

The transport modelling in MIKE SHE within the framework of SFL is closely related to the positions of discharge points from the deep bedrock, which have been calculated with the modelling tool ConnectFlow (Joyce et al. 2019). The calculated discharge points were concentrated to the biosphere object numbers 204 and 206, Figure 2-5. The objects are located close to the SDM MIKE SHE model boundary and it was decided to extend the SFL MIKE SHE model area to the north (Figure 2-5) in

order to avoid boundary effects when analysing the flow paths from the bedrock into the surface systems. The local model area used in the particle tracking simulations is marked in Figure 2-5 and defined by the sub-catchments of object 204 and 206.

Due to the extension of the model area, one new branch in the MIKE 11 model was added to the model. This small stream drains the agricultural area of object 204 and connects it with the mire in object 203.

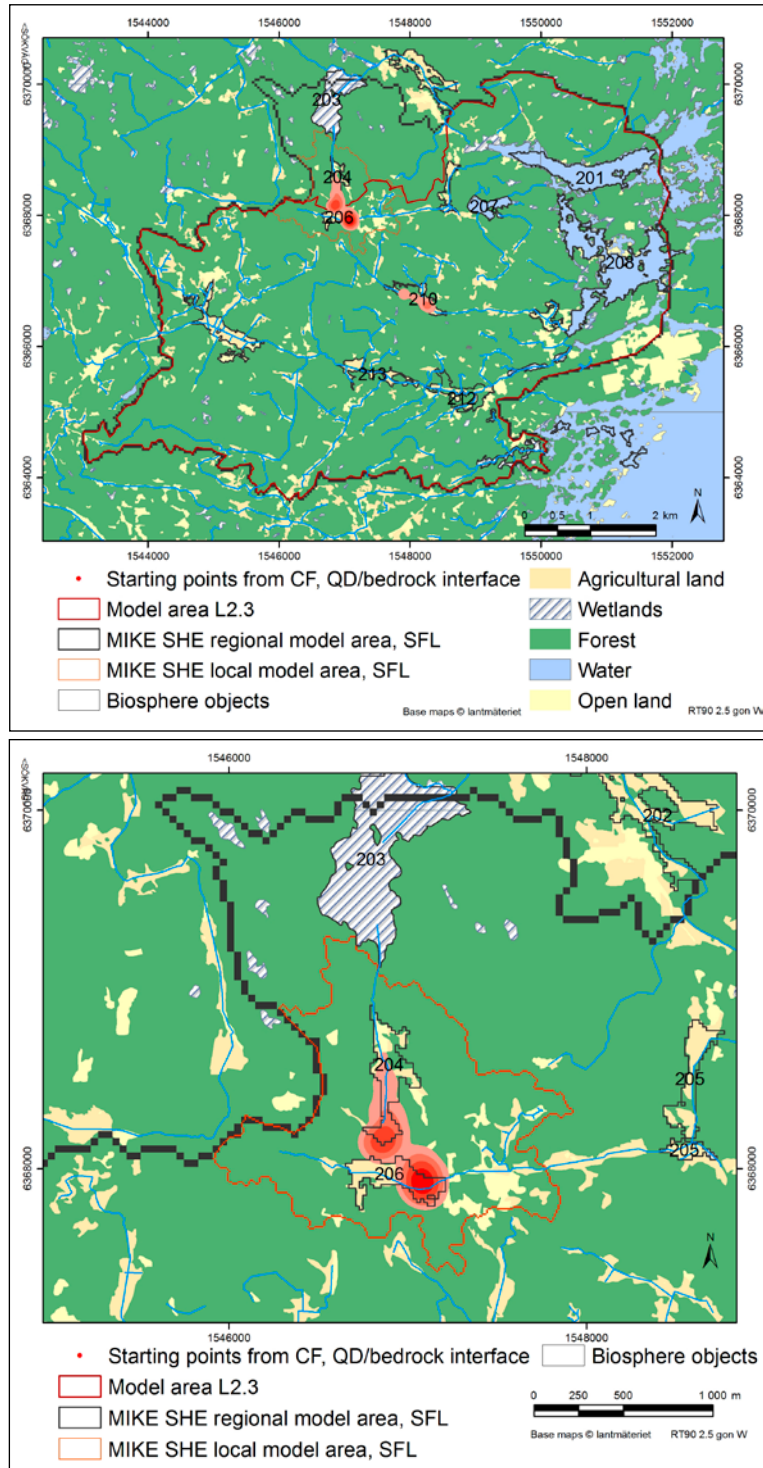


**Figure 2-5.** The L2.3 MIKE SHE model area, the SFL regional and local model area (upper figure). In the lower figure the local model area is shown in more detail with biosphere objects 204 and 206 and particle exit locations from ConnectFlow. The particle locations are represented as particle density plots, where light red corresponds to few particles and dark red to a high density of particles.

### 2.3.2 Flow modelling

MIKE SHE separates numerical calculation layers from geological layers in the saturated zone, see Figure 2-6. Geological layers are defined based on the stratigraphy of the QD and the bedrock geology. Calculation layers can be equal to the geological layers, or they may be defined independently. A calculation layer can have a smaller thickness than the defined geological layers, or it may consist of several geological layers. Also, the thickness of the calculation layer may be spatially varying. However, only the uppermost calculation layer in the saturated zone interacts and exchanges information with the unsaturated zone model. Consequently, if the upper calculation layer is too thin, the influence of evapotranspiration processes on groundwater dynamics may be underestimated. In order not to underestimate the evapotranspiration, the bottom of the upper layer should be below the phreatic surface (i.e. the groundwater table).

In the previous modelling with MIKE SHE in the Forsmark and Laxemar areas, it was concluded that the uppermost calculation layers has to be at least 2–2.5 m thick in order to capture all the surface processes influencing the subsurface. In all previous models, the thickness of the upper layer was constant all over the model area. The properties for a calculation layer are automatically calculated by MIKE SHE and averaged over the geological layers enclosed by the numerical calculation layer, for details see Bosson et al. (2009).

However, for transport modelling of radionuclides, it is desirable to have advective flows between all the geological layers in order to be able to follow accumulation along the flow paths through geological layers with different physical and chemical properties. Moreover, for dose modelling, a hydrological description of the uppermost biological active layer, where plant root uptake occurs, is of key importance. Therefore this work focuses on developing a method for following hydrological fluxes through each separate geological layer as far as possible, while still maintaining a fair representation of the effects of evapotranspiration on groundwater dynamics. Figure 2-7 shows the thicknesses of each QD layer, named Z1–Z6, in the Laxemar area, i.e. the MIKE SHE geological layers. Z1 is the uppermost layer following the same horizontal distribution as the map of QD. Z2 represent the surface peat in the terrestrial areas, and a hypothetical gravel layer in marine areas. Z3 is the gyttja-clay layer and the sand and gravel is enclosed in Z4. Z5 consists of glacial clay and Z6 is the till layer.

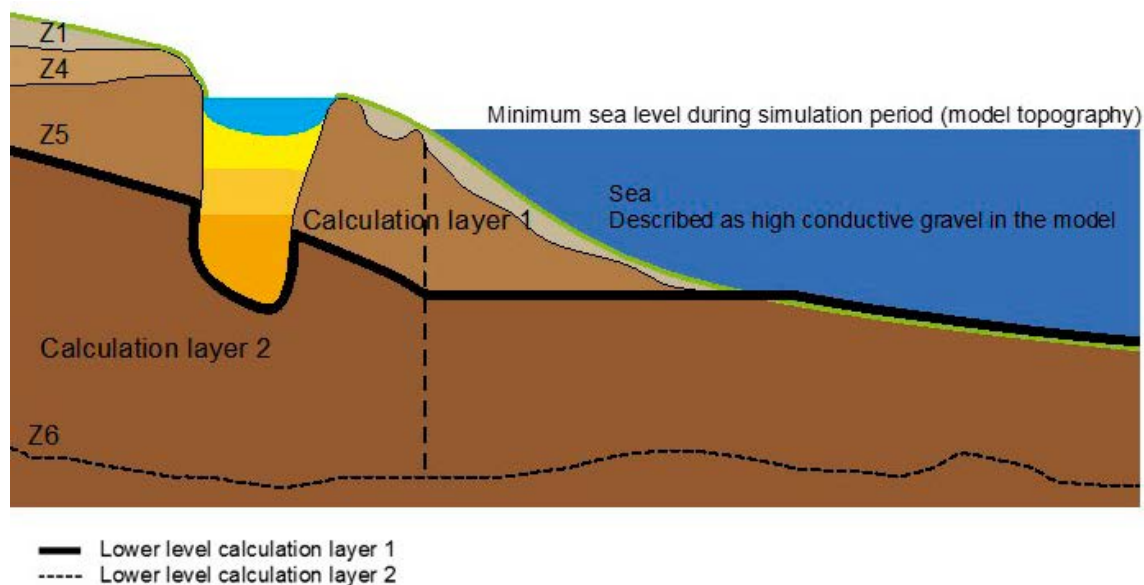


**Figure 2-6.** Schematic illustration of difference between MIKE SHE geological layers (Z1–Z6) and calculation layers.

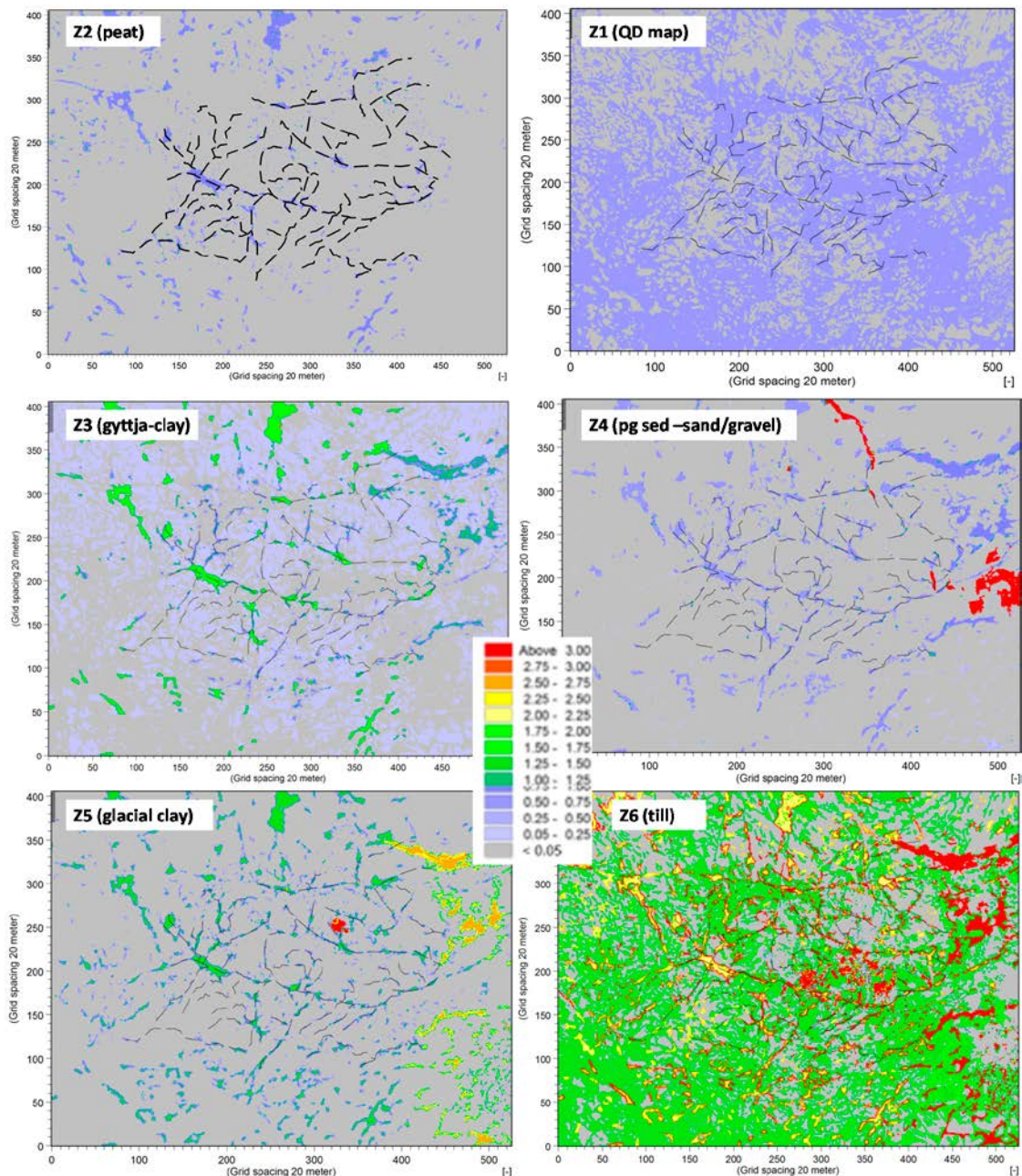


**Figure 2-7.** Thicknesses of Quaternary deposits (dotted lines are streams within the regional MIKE SHE model area). The Z1 and Z2 layers are surface layers.

Three methods for describing the uppermost calculation layer were tested on the Laxemar SDM-Site model:

### Groundwater table based alternative (Alt1)

In the first alternative, the annual average groundwater table was used for defining the uppermost calculation layer; this alternative is in the following referred to as Alt1. The annual average groundwater table was calculated based on a simulation with climatic data from October 2003 to December 2007. In areas where the annual mean groundwater table was located at a depth less than 1.9 m below soil surface, the thickness of the upper calculation layer was set to 0.1 m below the groundwater table. In areas where the groundwater table was deeper than the 1.9 m, the thickness was set to 2 m. Furthermore, in areas with surface water, the bottom of the upper layer was set to the lower level of the peat layer (Z2). The lower boundaries of calculation layers below the uppermost layer follow the lower levels of the geological layers Z4 to Z6. In total, Alt1 then has 4 calculation layers in the QD. Figure 2-8a shows the thickness for calculation layer 1 for Alt1.

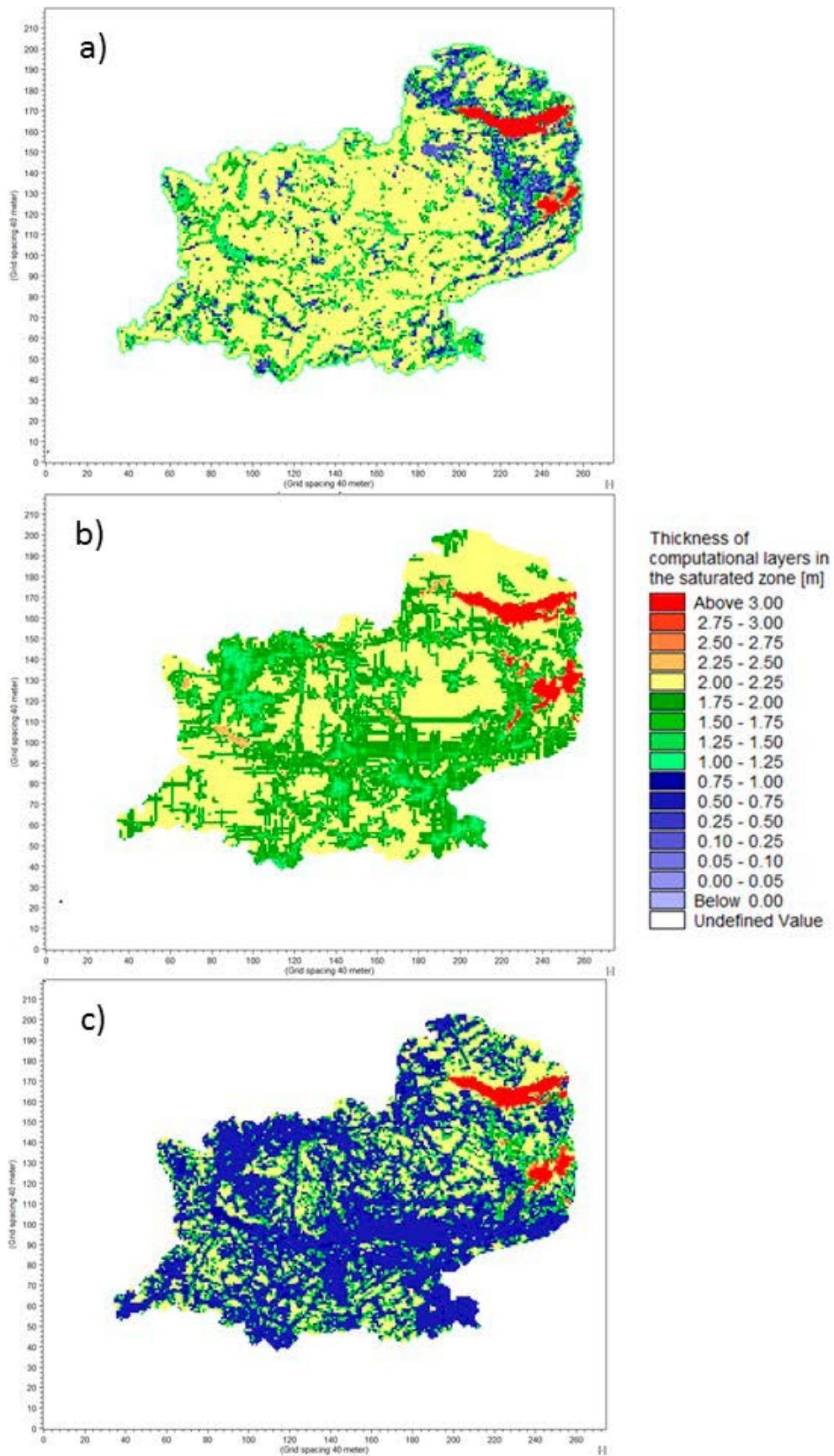


**Figure 2-8.** Thickness in meters of the uppermost calculation layer for the three alternatives; a) Alt1, which is based on the location of the annual average groundwater table, b) Alt2, based on layers down to and including the gyttja-clay, and c) Alt3, which only consist of the surface layer (Z1/Z2). For both Alt1 and Alt2 the thickness is 2 m in areas with bedrock outcrops.

### Gyttja-clay based alternative (Alt2)

The second option is based on the gyttja-clay layer and is in the following text referred to as Alt2. In Alt2, the three upmost geological layers i.e the surface layer, the peat and the gyttja-clay (Z1, Z2 and Z3) were lumped together. In all areas where the thickness of Z1–Z3 was greater than 1 m, the bottom of the upper calculation layer follows the lower level of Z3. Since Z2 and Z3 are mainly present in the valleys, i.e. in areas with shallower groundwater depths, a thickness with a minimum of 1 m was considered to be sufficient in those areas. In areas with bedrock outcrops, the thickness was set to 2 m. For the areas in between the valleys and the bedrock outcrops, where the sum of Z1, Z2 and Z3 did not exceed 1 m, the thickness of the upper calculation layer was interpolated from the thickness of the surrounding cells. As for Alt1, the lower boundaries of calculation layers below the uppermost layer follow the lower levels of the geological layer Z4 to Z6. Consequently, Alt2 also has 4 calculation layers in the QD. Figure 2-8b shows the thickness for calculation layer 1 for Alt2.

### Surface layer based alternative (Alt3)

In the third option, in the following referred to as Alt3, only the uppermost geological layer, the surface layer (Z1) or the surface peat (Z2), were combined into the uppermost calculation layer. In all areas where there are no bedrock outcrops, the thickness of calculation layer 1 is the thickness of Z1+Z2. In areas with bedrock outcrops, the thickness was set to be 2 m. The lower boundaries of calculation layers below the uppermost layer follow the lower levels of the geological layers Z3 to Z6. In total, Alt3 then has 5 calculation layers in the QD. Figure 2-8c shows the thickness for calculation layer 1 for Alt3.

A comparison of the thickness of the uppermost calculation layer shows that, on the average, Alt3 has the thinnest layer, with more than 50 % of the model area thinner than 1 m (Figure 2-8, Table 2-4). In Alt1 there are areas with a thickness of less than 1 m as well, but only in about 11 % of the area, Table 2-4. In Alt1, almost 2/3 of the area has a thickness greater than 2 m. Alt2 has no areas at all with a thickness less than 1 m. Instead, the thickness for Alt2 is almost evenly distributed between a thickness between 1 m and 2 m and a thickness greater than 2 m.

The local model (See Section 2.3.1 and Figure 2-5) followed the same vertical discretization as Alt2 above. The horizontal boundary conditions were defined by exporting time varying fluxes of groundwater from the regional model to the local model boundaries. The top and bottom boundary conditions were the same as in the regional model, i.e. a no-flow bottom boundary condition at 600 m depth and precipitation and potential evapotranspiration as top boundary condition.

**Table 2-4. Resulting thicknesses of the uppermost calculation layer in percentages of the total model area for the three alternatives Alt1 to Alt3.**

Thickness (in % of total area)	Alt1	Alt2	Alt3
< 1 m	11	0	54
1–2 m	25	47	21
> 2 m	64	53	25

### 2.3.3 Transport modelling

Particle tracking (PT) simulations were only performed in the local model, aimed at analysing the groundwater flow paths in the QD. Particles released within the volume of the generic SFL repository were traced through the bedrock in the hydrogeological model ConnectFlow (Joyce et al. 2019). Particle positions from these flow paths at the bedrock/QD interface were imported to the MIKE SHE local model and further traced in the surface systems in three different cases PT1, PT2 and PT3 (Table 2-5). The main part of the particles released in the SFL repository discharge in biosphere object number 204 and 206 (Figure 2-5). Consequently, the flow paths analysis in MIKE SHE was focused only on the particles discharging in those objects.

In MIKE SHE, where PT is calculated with a local velocity vector method, the exact starting point of a particle cannot be defined. Only the cell, and at which level within that cell, the particle should be released can be specified. The particle locations at the QD/bedrock interface from ConnectFlow were imported to the MIKE SHE model. The particles are introduced in the QD/bedrock interface zone, approximately 2 m below the till layer. With the aim to capture potential differences in the flow field between the two models, the calculated particle density from ConnectFlow was not considered. Instead, all cells containing any ConnectFlow particles were in MIKE SHE assigned an initial concentration of 500 particles in Case PT1. By applying the same number of particles in all cells in the QD/bedrock interface, the particle density at ground surface calculated in MIKE SHE is not biased by the particle density calculated in ConnectFlow. The reason for the high number of particles per cell is to capture the main flow direction from each cell. E.g. by introducing one randomly placed particle per cell, the particle may get a flow path direction not representative for that cell due to numerical dispersion. The particles were traced for 1 000 y in a transient flow field describing inter-annual variations. The year 2006 were cycled 1 000 times.

In addition to the simulation case described above (PT1), where all particles from Connectflow within the local MIKE SHE area were included, two simulations focusing on particles in or close to the border of Biosphere object number 206 were performed. The year 2006 were cycled 1 000 times also in those cases. The particle locations from ConnectFlow in the QD/Bedrock interface were analysed and only the areas with highest concentration of particles, according to the density plot shown in Figure 2-5, were further traced in MIKE SHE. I.e. single cells hit by only a few particles were not assigned an initial concentration of particles in the MIKE SHE PT-simulation. The aim with this simulation, named PT2, was to analyse the travel times and flow paths pattern through each single type of QD in detail. A sensitivity case of the Case PT2-simulation was run, named Case PT 3, aiming at analysing the influence of total porosity on the particle travel times. In the MIKE SHE SDM-modelling, the total porosity values used for PT modelling were assumed to be equal to the Specific yield values used in the flow modelling (Table 2-2 and Table 2-3). This “MIKE SHE SDM-approach” was applied in PT1 and PT 2. The Specific yield values for till, glacial clay and clay-gyttja/gyttja clay in Table 2-2 and Table 2-3 are low and does not represent a proper estimate of the total porosity, which is the sum of specific yield and specific retention (Bear 1979). With the aim to analyse the influence of total porosity on flow paths lengths and travel times, higher total porosity values for till, glacial clay and gyttja-clay/clay-gyttja were applied in Case PT3. For this sensitivity case, site specific data was not used, instead a representative value from literature data was applied to the model (Morris and Johnson 1967). The three particle tracking cases are described in Table 2-5 and starting positions are visualized in Figure 2-9. The porosity values used are listed in Table 2-6.

**Table 2-5. Particle tracking cases performed in MIKE SHE. For both cases initial positions were imported from the ConnectFlow calculations (Joyce et al. 2019).**

Case	Simulation period (years)	Number of cells with initial concentration of 500 particles
PT1	1000	257
PT2	1000	105
PT3*	1000	105

\* Porosity values according to Table 2-6.

**Table 2-6. Specific yield (-) and Porosity (-) values for till, gyttja-clay/clay-gyttja and glacial clay used in the Particle tracking Case PT1, 2 and 3. In PT1 and 2 the total porosity was assumed to be equal to the specific yield values applied in the flow modelling (Table 2-2 and Table 2-3).**

QD	PT1 and PT2	PT3
Till	0.05	0.45
Gyttja-clay/clay-gyttja	0.03	0.4
Glacial clay	0.25	0.4

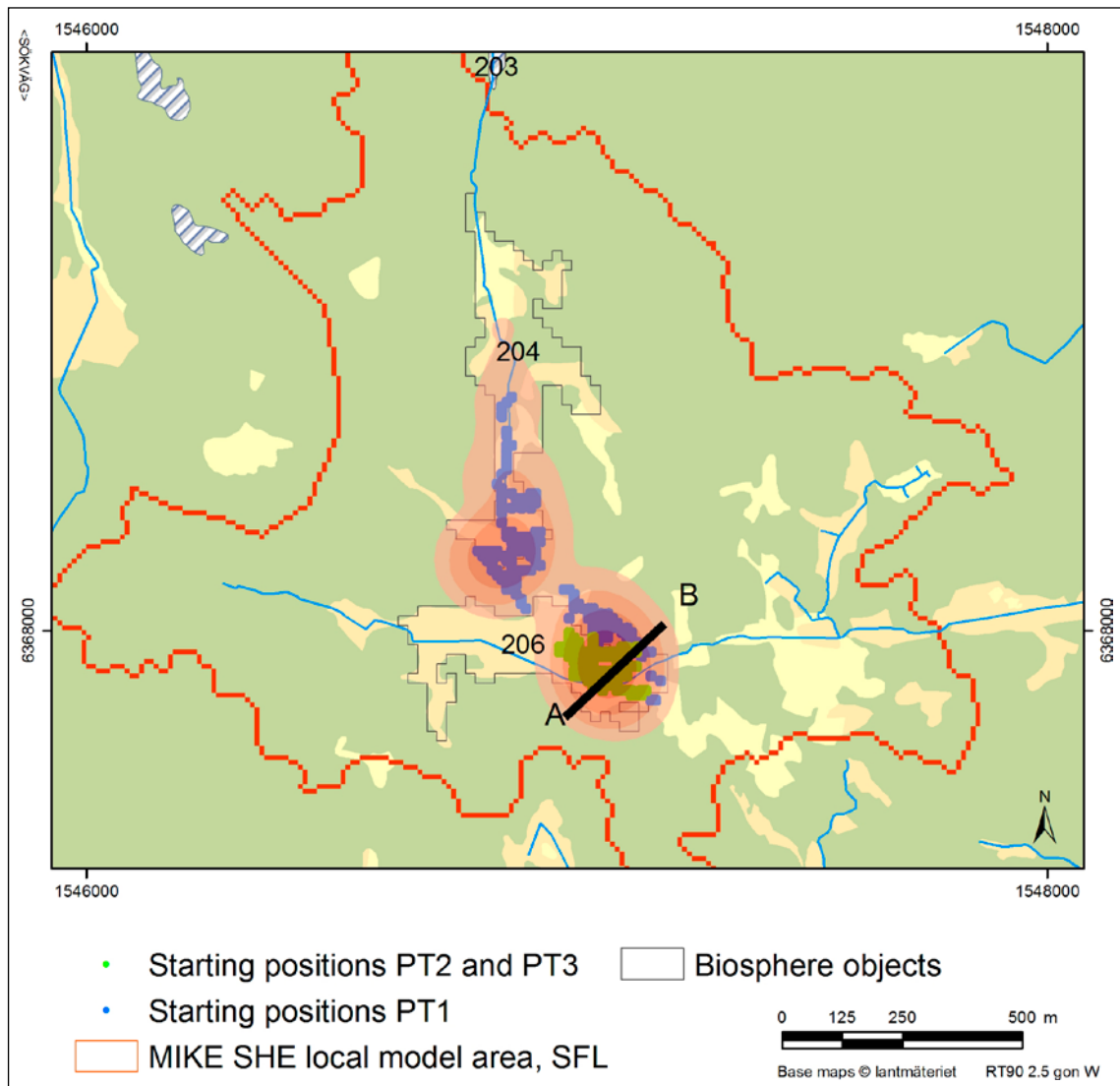


**Figure 2-9.** Initial particle locations in simulation Case PT1, PT2 and PT3. The particle density in the QD/Bedrock interface calculated in ConnectFlow is illustrated as a transparent layer.



## 3 Results

### 3.1 Sensitivity analysis of numerical implementation of geological soil layers

Simulations for the alternatives Alt1–Alt3, as described in Section 2.3.2, were made for the period from October 2003 to December 2007. Results from the simulations were extracted in order to see whether any of the alternatives were comparable with results from the original SDM Site model. The aim was to reach as good as or better results than the L2.3 MIKE SHE model, in terms of surface discharges and groundwater levels.

The first results evaluated were the regional water balances, i.e. the water balances for the entire land part of the model domain. A comparison of the results showed that the overall numbers for the total evapotranspiration and surface runoff were very similar between the original model and Alt1 and Alt2. For Alt3, the total evapotranspiration was approximately 90 % of the original model, and consequently the runoff for Alt3 was about 10 % higher for Alt3. Analysing the water fluxes in the bedrock, the differences are small between all models, and especially at lower depths.

Results were also extracted for the surface streams and comparisons of the results showed that the accumulated discharge over the 3-year period was very similar for alternatives Alt1 and Alt2 compared to the SDM Site results, while Alt3 yielded a higher accumulated discharge in all observation points. The difference varied between 5–15 % for the 4 discharge observation points. The reason for the higher discharge is the larger runoff due to less evapotranspiration in Alt3, which is an effect of an upper calculation layer that is too thin in parts of the model.

For the groundwater observation points, a comparison between the ME (mean error) and MAE (mean absolute error) was made for the SDM-Site model and the three alternatives. For the groundwater observation points (SSM wells), results were compared both for saturated zone head elevation and for depth to phreatic surface. For the bedrock monitoring points, the results are illustrated for head elevations. Table 3-1 shows the average MAE and ME values for the SDM Site model and for the three alternatives Alt1, Alt2 and Alt3. The SDM Site values may differ from the values reported in Bosson et al. (2009) because in this study the average MAE and ME values are based on all the observation points both for head and depth, while in Bosson et al. (2009), the average MAE/ME values are based on either head or depth for each point.

For the groundwater observation points in the soil (the SSM wells), the average MAE for the SDM Site model was 0.55 when evaluated as head, and the average ME was 0.17. All of the three alternatives had similar MAE values, although slightly higher. The ME values however, were close to zero for both Alt1 and Alt2 while Alt3 differed significantly. A positive ME value means that the modelled values on the average are lower than measurements. When evaluating the SSM wells with regard to depth to phreatic surface instead of head elevations, the average MAE for Alt1 is very close to the SDM Site value, but lower for both Alt2 and Alt3. The corresponding ME values are close to zero for both Alt1 and Alt2, while further from zero for Alt3. For the bedrock monitoring points, the average MAE are similar in all simulation cases, while the ME is positive for all cases except for Alt3, which has a negative average ME close to zero.

**Table 3-1. Average MAE (m) and ME (m) for the SDM Site model and for the three alternatives.**

	SDM Site		Alt 1		Alt 2		Alt 3	
	MAE	ME	MAE	ME	MAE	ME	MAE	ME
SSM wells, head	0.55	0.17	0.58	0.05	0.61	-0.06	0.63	-0.37
SSM wells, depth	0.92	0.12	0.93	-0.01	0.66	0.09	0.71	-0.28
HLX, head	1.05	0.48	1.01	0.36	1.01	0.30	1.01	-0.13
Total, average	0.84	0.25	0.84	0.13	0.76	0.11	0.78	-0.26

In general, the average MAE values are similar or lower for all three alternatives than for the SDM Site model. The ME values are significantly closer to zero for both Alt1 and Alt2. For Alt3, the ME values are all negative, which may be an effect of the underestimation of the evapotranspiration due to too thin upper calculation layer.

Simply looking at the average MAE or ME values gives an indication of how well a model performs but it does not give any information about individual measurement points. In the present evaluation of results, 33 observation points in the regolith, evaluated both as head elevations and depth to phreatic surface, and 50 observation points in the bedrock were used for comparisons between four models. Because of the high number of observation points to be evaluated, it is difficult to interpret the results based on all MAE/ME values individually. Instead, scatter plots for both the MAE and the ME values were made, see Figure 3-1. Each MAE and ME value for the alternative models was compared to the corresponding value from the SDM Site model; the 1:1 line indicates equal values between SDM Site and alternative models. Figure 3-1a), c) and e) shows the MAE for the SSM points head, SSM points depth, and HLX points, respectively, and Figure 3-1b), d) and f) the corresponding ME values. None of the three alternatives follow the 1:1 line but in all figures it is clear that Alt3 differs more than Alt1 and Alt2.

An alternative to the scatter plots for the MAE values, as illustrated in Figure 3-1, is to normalize the MAE values for the alternative models with the SDM Site MAE. A ratio close to 1 means that the alternative model and the SDM Site model have similar MAE values, i.e. the fit to measurements is the same. It does not necessarily imply that the fit to measurements is good, just that it is as good as for the SDM Site model. Consequently, a ratio diverse from 1 could mean both a better or worse fit to measured values. However, plotting the ratio for each observation point is an illustrative way to identify which alternative is closest to the SDM Site results. Figure 3-2 is showing the ratio between each of the three alternatives and the SDM-Site model MAE values.

In the upper panel in Figure 3-2, MAE ratios for the head elevations in the SSM observation points are illustrated. In the middle panel, MAE ratios for the depth to the phreatic surface are shown, and in the lower panel the MAE ratios for the head elevations in the bedrock are illustrated. In general, it may be noted that the largest discrepancies are found for Alt3, although there are points with opposite results as well.

For the ME values, the ratio as presented in Figure 3-2, is not as easy to plot since there may be both positive and negative values for each observation point. In the Appendix, all values for MAE and ME are presented.

Interpreting results for the groundwater observation points in terms of MAE or ME values is usually not enough since an average value does not necessarily reflect the correct pattern of a time series graph. It is important that not only the average elevation or depth is correct but also the seasonal pattern of each observation point. Figure 3-3 gives a few examples of time series graphs for observation points in the QD. The observation points were mainly selected in order to show that it is not always straightforward in deciding which alternative give the best agreement. In the upper figure, representing the head elevation from position SSM0021, Alt1 and Alt2 both give similar results to the SDM Site model, while Alt3 does not follow the seasonal pattern as good as the others. In the middle figure, Alt2 gives the best results since it captures the amplitude of the measurements more accurately, while neither Alt1 nor Alt3 manage to reflect the seasonal pattern. In the lower figure, Alt1 gives the best result of the three alternatives. As seen in the graphs, it is not obvious that one of the alternatives always gives the best results. However, Alt3 seem to give the poorest results in most cases.

Based on the results illustrated in this section, it was concluded that Alt1 and Alt2 are both able to describe measurements in a comparable way to the SDM Site model. The results from Alt3 are not satisfactory in several ways since both the water balance results differ from the SDM Site water balance and the MAE and/or the ME values are in many case significantly higher than the SDM Site results, indicating a weaker fit to field measurements. Whether the layer description according to Alt1 or Alt2 should be used may be decided based on the model area and problem description to solve. In this study, Alt2 was chosen because it is focusing on the regolith layers rather than the groundwater levels, and also because the results for the MAE/ME was slightly better than the other two alternatives.

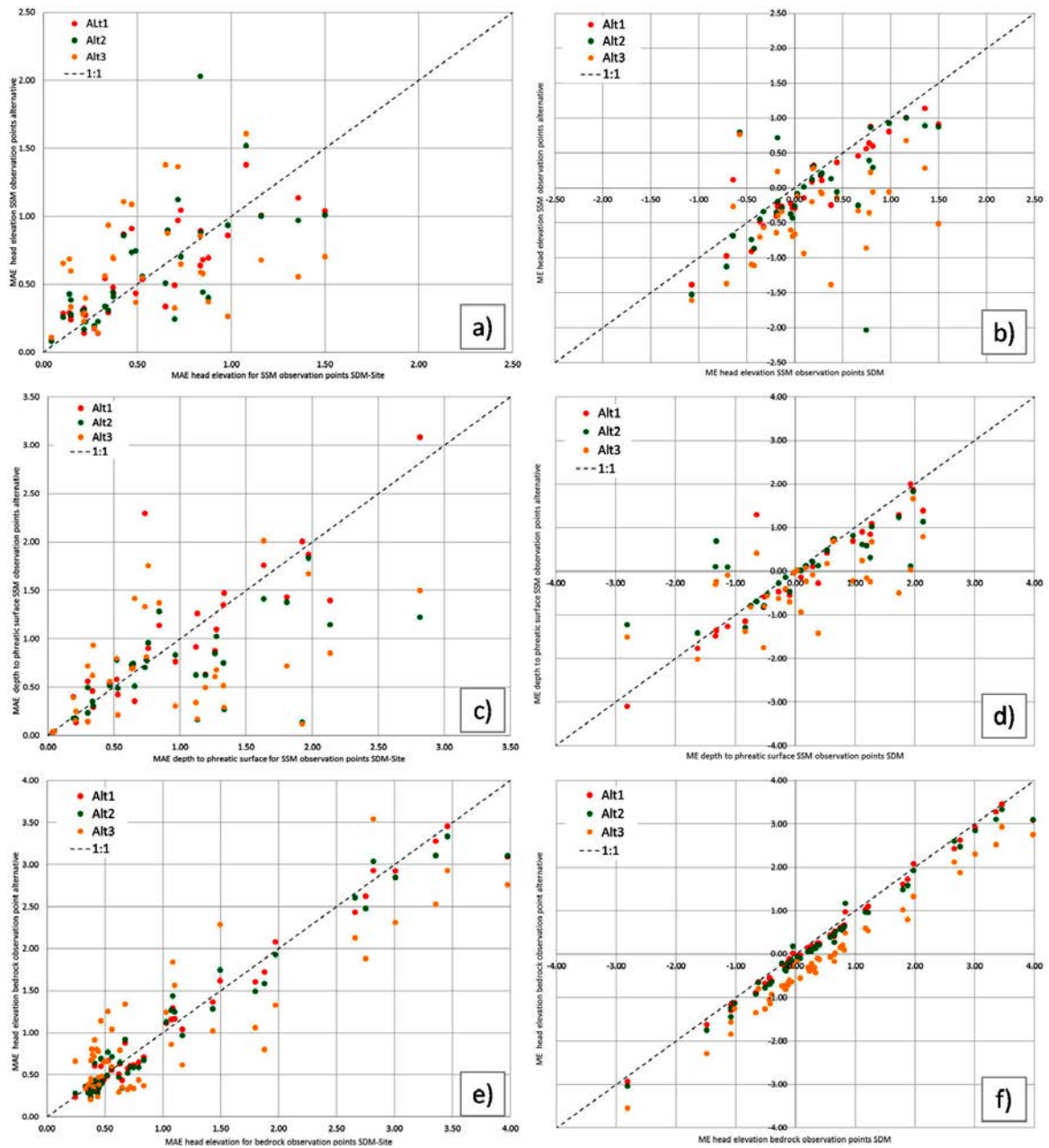


**Figure 3-1.** Scatter plots comparing the MAE and ME for the three alternative models, Alt1–Alt3, with the SDM Site; the figures are illustrating a) MAE for the SSM observation points evaluated as head elevation, b) the corresponding ME values, c) MAE for the SSM observation points evaluated as depth to phreatic surface, d) the corresponding ME values, e) MAE for the bedrock monitoring points, and e) the corresponding ME values. In all graphs, the results for the alternatives are illustrated on the y-axis, while the SDM Site values are illustrated on the x-axis.

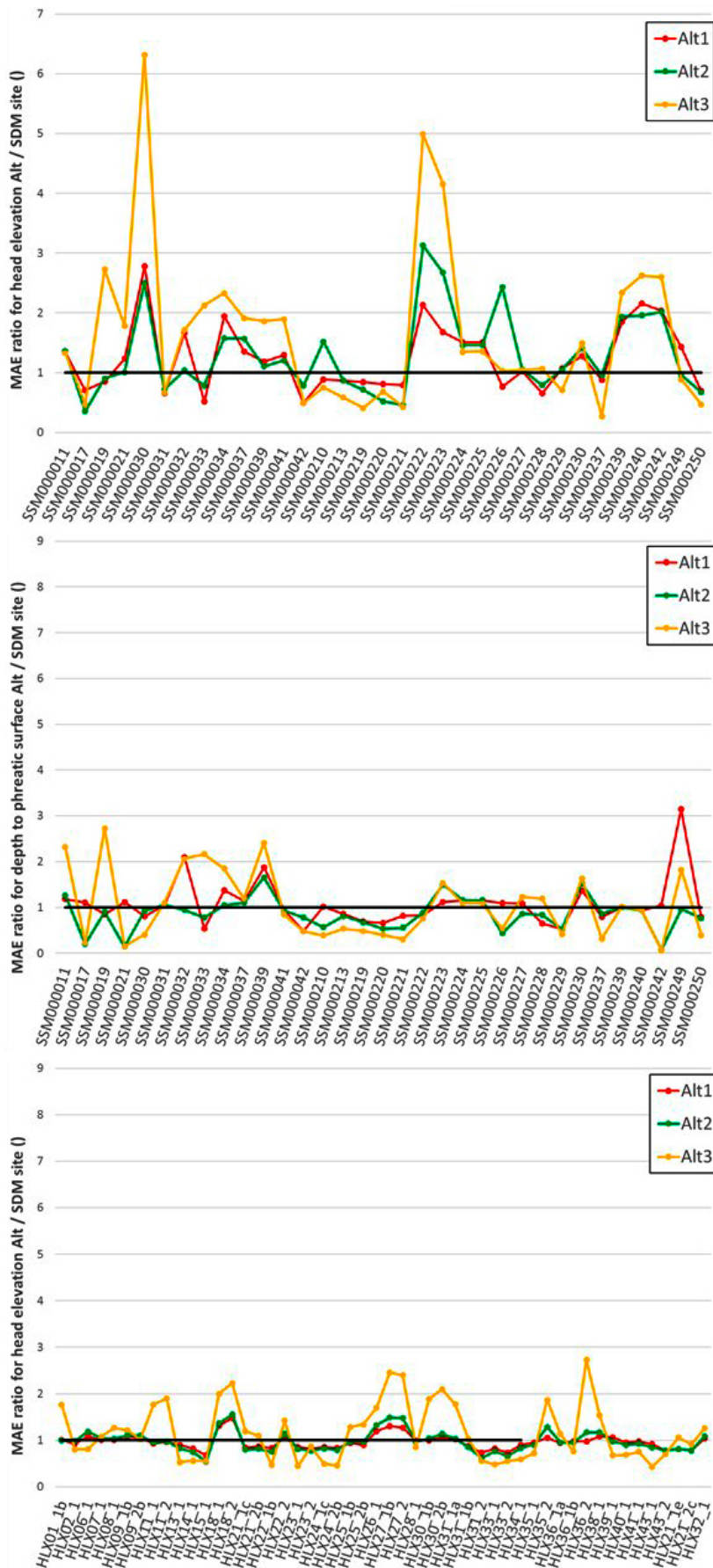


**Figure 3-2.** Ratio between MAE results from the three alternatives Alt1–Alt3 and the MAE for the final SDM-Site model for each observation point.

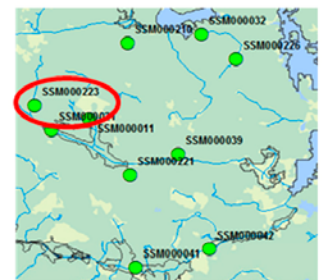
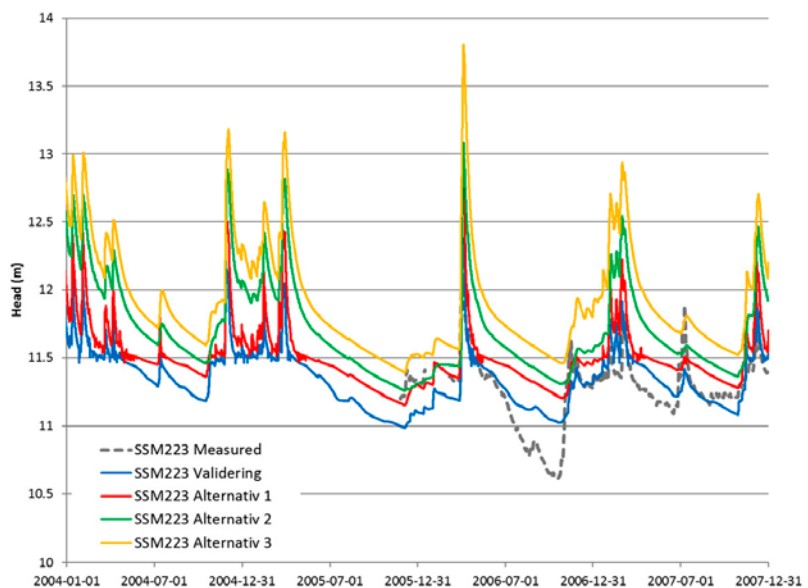
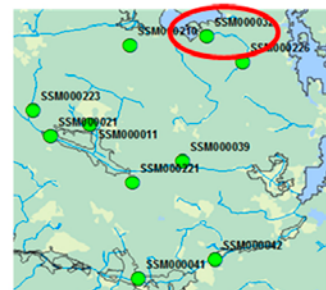
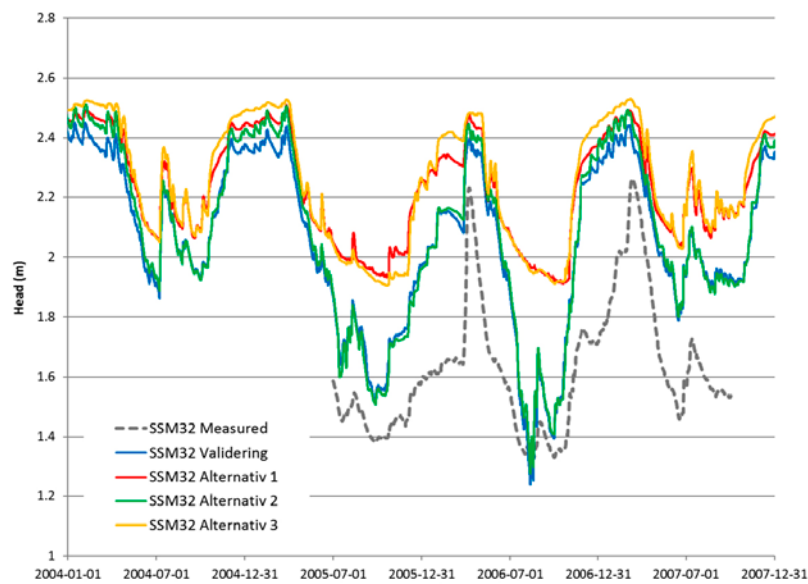
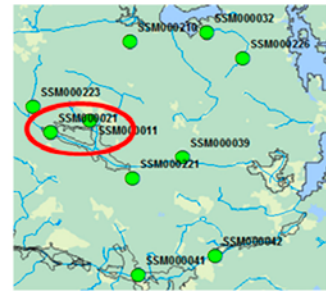
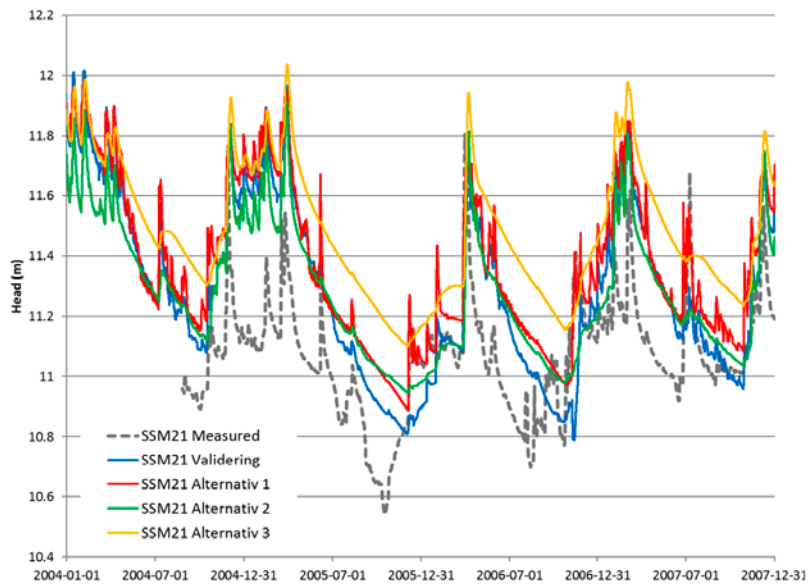


**Figure 3-3.** Example of time series for three different groundwater observation points. The head elevation predicted by the SDM-Site model (blue line), and the three alternative models Alt1 to Alt3 (red, green and yellow) are compared to field measurements (grey dashed line).

### 3.2 Transport modelling in local model

The results from Case PT1, PT2 and PT3 were evaluated in terms of exit locations and sinks on the ground surface and total flow paths length and travel time from bedrock to each sink. In MIKE SHE the particle tracking simulation is only possible in the saturated zone. Thus, when the particles leave the saturated zone the position and the type of sink is registered and the particle is not further traced. Table 3-2 summarizes the results from the three cases. In all cases approximately 30 % of the particles discharge to the unsaturated zone and 70 % of the particles go to the stream network. The exit location of the particles reaching the unsaturated zone is not concentrated to the stream network, rather to the slight hill slopes surrounding the agricultural areas.

**Table 3-2. Number of particles and different sinks in Case PT1, PT2 and PT3.**

	PT1	PT1_%	PT2	PT2_%	PT3	PT3_%
Initial number of particles	128 500	100	52 000	100	52 500	100
Particles left in the model volume after 1000 y	2 061	2	0	0	31	0
Particles gone to Unsaturated zone	44 427	35	13 944	27	15 556	30
Particles gone to river network	82 012	64	38 556	74	36 913	70

In Cases PT1 and PT2 approximately 40 % of the particles have travel times between 1–2 years and in Case PT 3 approximately 40 % of the particles have travel times between 2–5 years. In all cases the majority of the particles have relatively short flow path lengths between 20–75 m. The distribution of travel times and flow paths lengths are similar in the three cases, Figure 3-4 to 3-6 illustrate the relative distribution of flow paths lengths and travel times of the released particles for each case.

The particles in Case PT1 have the longest flow paths registered. Particles with long and slow flow paths are particles not introduced in distinct discharge areas and some have captured a downward flow path into the bedrock. 2 % of the introduced particles are still left in the model volume after 1 000 y (Table 3-2), and the same portion of particles have travel times longer than 10 years (Figure 3-4).

In Case PT2 both the maximum flow path lengths and the travel times are shorter than in PT1. No particles are left in the model volume at the end of the simulation. The reason to shorter and faster flow paths is that the particles in PT2 are only introduced in distinct discharge areas. In PT1 particles were released in all cells where a flow path from ConnectFlow crossed the cell, with no regard to the concentration of particles. Also, local recharge and discharge conditions in the QD/bedrock interface zone captured in MIKE SHE might not have been identified in ConnectFlow. A few particle traces from the deep bedrock ends up in local recharge areas according to the hydrological conditions calculated in MIKE SHE. The particles released in these areas are the 2 % found in the bedrock at the end of the PT1 simulation. In Case PT2, the longest flow path from start position to a sink at the ground surface (river or unsaturated zone) is 140 m and the median flow path is 42 m, compared to 400 m and 54 m in Case PT1. The longest travel time is 4 560 days and the median travel time is 690 days, i.e. approximately 2 years, Figure 3-5.

The travel flow paths are not strongly influenced by the increased porosity applied to the different QD-layers in PT3 with a maximum length between source and sink of 159 m and a medium flow paths lengths of 46 m. However, the travel times increase significantly with the median travel time increasing from 689 days in Case PT2 to 1 820 days in Case PT3, Figure 3-6. The maximum travel time in PT3 is approximately 200 years compared to a maximum travel time of approximately 10 years in PT2.

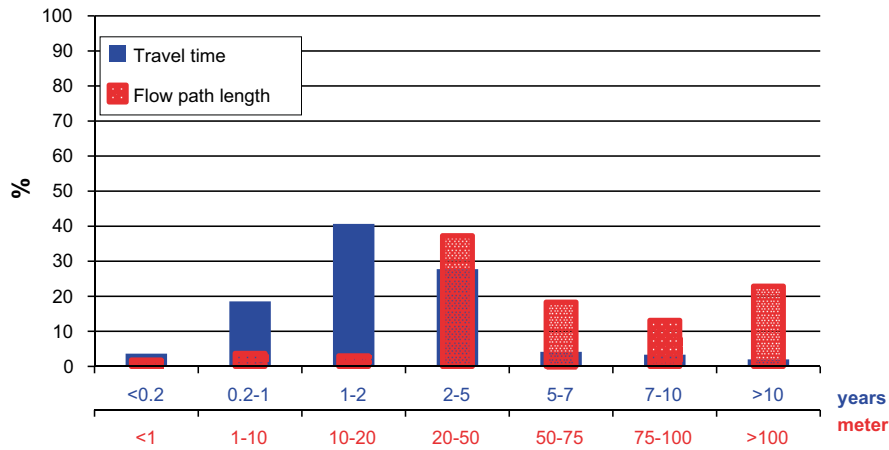


**Figure 3-4.** Relative distribution of travel time and flow paths length for particles released in Case PT1. The total number of released particles in PT1 was 128 500.

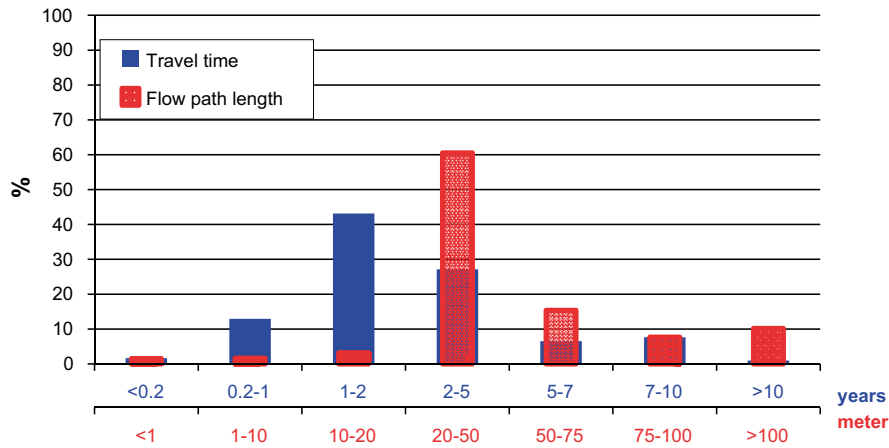


**Figure 3-5.** Relative distribution of travel time and flow paths length for particles released in Case PT2. The total number of released particles in PT2 was 52 500.

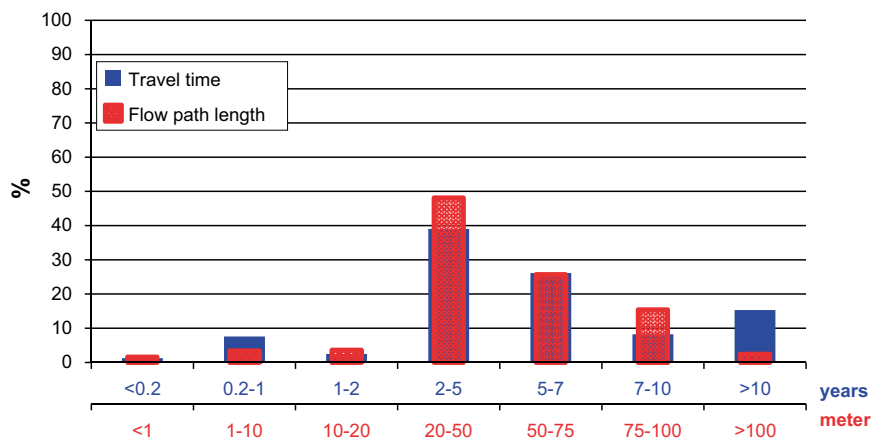


**Figure 3-6.** Relative distribution of Travel time and flow paths length for particles released in Case PT3. The total number of released particles in PT3 was 52 500.

The travel times and flow paths of particles released in PT2 are illustrated in 3D in Figure 3-7. The overall flow path pattern is the same in all cases, thus only Case PT 2 is illustrated with a 3D figure. In Figure 3-7 only the particles registered in the sink “unsaturated zone” are visualised. The particles are introduced in the QD/bedrock interface zone, approximately 2 m below the till layer. The different QD layers are schematically marked with red dashed lines in the figure. As long as the particles are in the bedrock the transport is dominated by its vertical component. When entering the till, the horizontal transport component increases whereas the transport through the low conductive clay layer is predominantly vertical. When the particles enter the sand layer the horizontal transport increases again. The longest median travel time for all particles in one single QD-layer in Case PT2, 270 days, are found in the clay layer and the longest median flow path lengths, 23 m, is found in the sand layer for this case (Table 3-3). The travel times and flow paths lengths through the till layer are also relatively long, 193 days and 13 m. The shortest times and flow path lengths are found in the uppermost QD-layer i.e. the particles have a relatively short and quick way through the uppermost QD before they enter a stream or an area with unsaturated conditions.

In Case PT3 the longest travel times are found in the till and clay layer as in Case PT2. However, in this case the longest median travel time is found in the till layer and not the clay layer. Also, there is a strong increase in total travel times over all layers with the largest increase in the till layer. The largest changes in flow paths length are found in the till and the sand layer. The till flow paths length decreases and the medium flow path length in the sand is almost doubled.

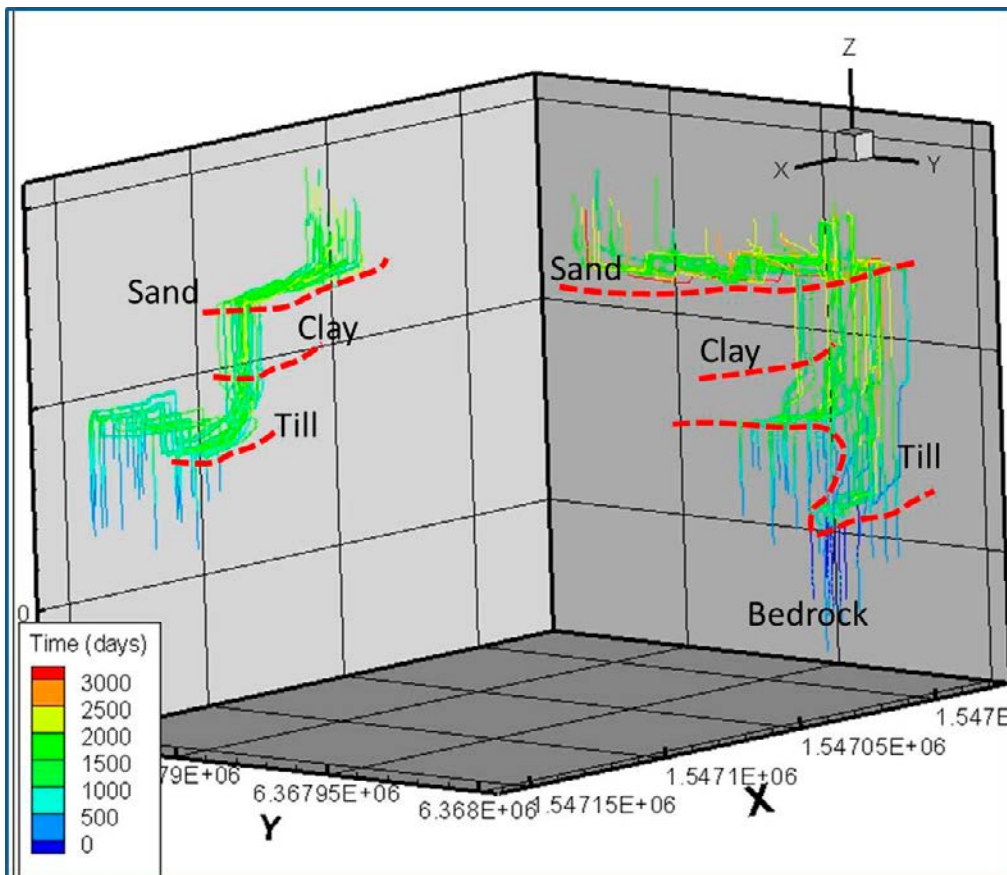


**Figure 3-7.** Particle flow paths from the QD/bedrock interface to the ground surface (PT2). The different QD-layers are schematically marked in the figure.

**Table 3-3. Median travel time and flow path length through each QD-layer in Case PT2 and PT3. Maximum values are written i bold.**

Layer	Median Travel time, days		Median flow path length, m	
	PT2	PT3	PT2	PT3
Bedrock_init	31	30	1	0.98
Bedrock/QD interface	34	69	1	2.38
Till	193	<b>821</b>	13	2.38
Clay	<b>270</b>	557	1	1.14
Sand	96	145	<b>23</b>	<b>39</b>
Uppermost QD	23	65	0.4	0.62

### 3.3 Converting information from Mike SHE to dose models

In the Forsmark SR-Site project (Bosson et al. 2010), a method was developed for delivering advective flows from the MIKE SHE model to the dose model. The flow from the bedrock and through the QD was estimated based on average water balances for six existing lake and mire areas within the MIKE SHE model area. In the Forsmark SR-Site model, the QD was described with only two calculation layers. The uppermost calculation layer was 2.5 m thick all over the model area. The second layer had a lower level following the bedrock model and consequently the thickness of the second layer varied extensively over the area. Figure 3-8 shows a schematic figure over how fluxes in MIKE SHE were translated into advective fluxes between regolith layers in a box model. The left side of the figure shows a fictitious cross section of a lake and mire area. Based on the MIKE SHE flow model, water balance results for any selected model area may be extracted. Also the period for which results should be extracted may be specified. In all of the water balances discussed in the following, extractions were made based on annual values.

Within the framework of the Forsmark SR-PSU project, it was desired to refine the methodology from the SR-Site (SSM 2018, Klos and Wörman 2015). Instead of averaging values for existing lakes, individual water balances were extracted for a number of the specified biosphere objects (Werner et al. 2013). Water balances were also extracted from three different models in time (3000 AD, 5000 AD, and 11 000 AD) representing different successional stages. However, although the number of calculation layers in the MIKE SHE model was increased from two to four layers, the calculation layers still did not follow the geological layers. The upper calculation layer was still 2.5 m thick, the second layer 1.5 m, the third 2.0 m and the fourth regolith layer was the remaining thickness of the regolith if thicker than 6 m, or had a minimum thickness of 0.5 m.

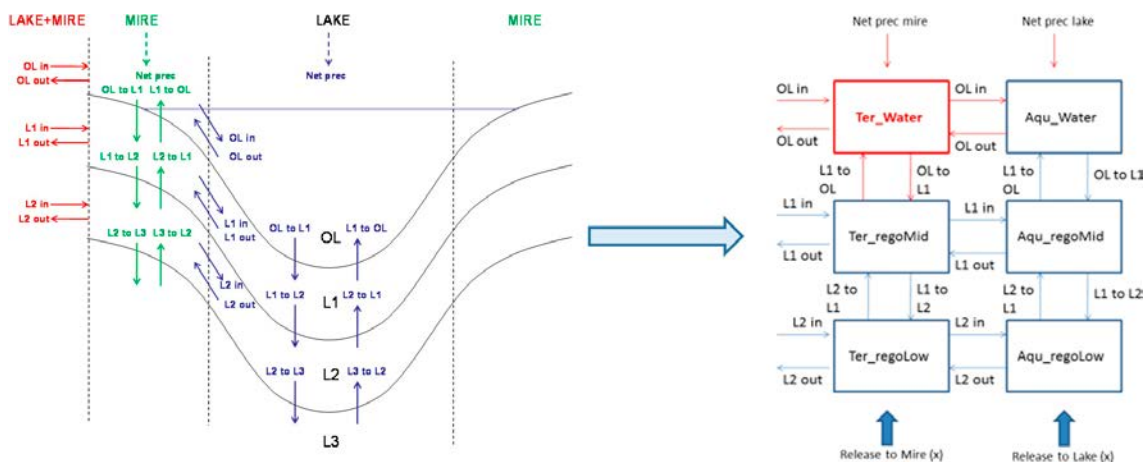


**Figure 3-8. Discharge components between different layers and compartments converted into a box model.**

Since the MIKE SHE calculation layers were different from the regolith layers in the radionuclide model, a method for mapping the water flows from one model to the other had to be invented. First, in the delivery from MIKE SHE to the radionuclide-transport modelling, the uppermost layer was divided into two layers, with thicknesses of 0.5 m and 2.0 m respectively. The near-surface groundwater flow was assigned to the upper 0.5 m layer, whereas other contributions are distributed according to relative thickness (20 % and 80 %).

Then, for the translation of vertical flows, each boundary between two regolith layers was mapped to the depth of the corresponding MIKE SHE calculation layers. Then the upwards and downwards vertical flows at the regolith boundary were calculated assuming that flows change linearly within MIKE SHE calculation layer. Figure 3-9 illustrates how the mapping and parameter extraction was made.

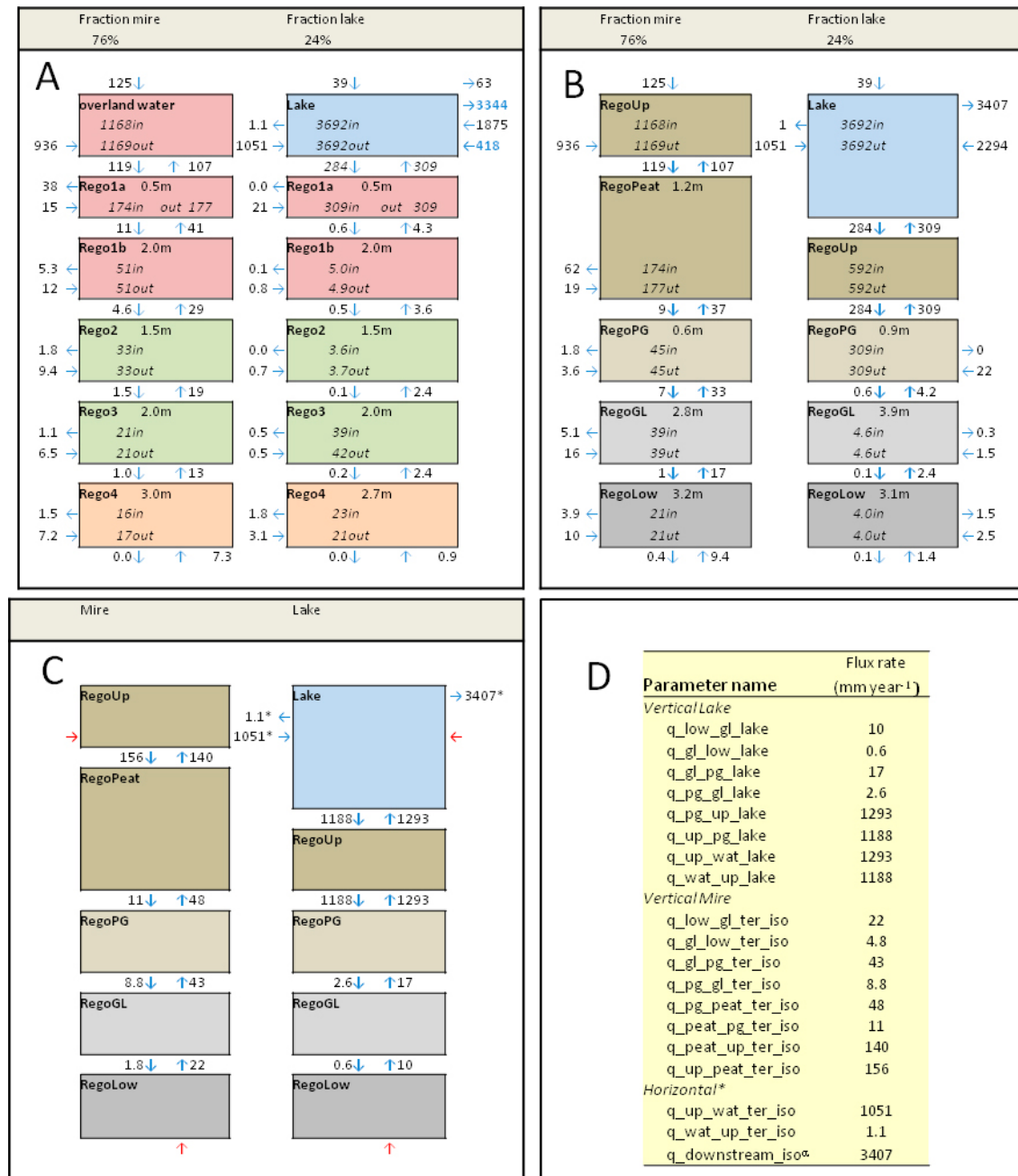


**Figure 3-9.** Transformation of water balance components into radionuclide model parameters (Werner et al. 2013) A) MIKE SHE-calculated water balance components for biosphere object 157\_2 in Forsmark. B) Estimated cross-layer fluxes. C) Fluxes delivered to the radionuclide transport modelling, scaled according to relative sizes of lake and mire areas. Red arrows represent potential release pathways for radionuclides. D) Parameter names and associated inter-compartment water fluxes used in the dose model.

In the upper left figure (A), the water balance from MIKE SHE is shown. The upper right figure (B) shows the flux rates between regolith layers after interpolation. The lower left figure (C) shows flux rates used in the radionuclide model scaled per area mire or lake. Horizontal flux rates between regolith layers were small in relation to the lateral spatial scale, and were neglected in the transport modelling. Finally, the lower right figure (D) show the parameter names used in the radionuclide modelling. More details on the mapping are found in e.g. Werner et al. (2013).

However, this method still requires a number of simplifications. In order to avoid too many steps with transformation of data, the next step in improving the transformation from MIKE SHE to the radionuclide model is to keep the geological layers in the MIKE SHE model as equal to calculation layers as possible. To examine the effect of thinner calculation layers, two objects of different types within the SDM Site model area were selected. Figure 3-10 shows the location of the two selected objects for which water balances were extracted both from the SDM-Site model and the three alternative models Alt1–Alt3. Object 207 is a lake area, Lake Frisksjön, and consequently under saturated conditions during most weather conditions. Object 212 is an area with deciduous forest surrounding arable land along water streams, and therefore more sensitive to climatic conditions.

Results are presented in Figure 3-11 (object 207) and Figure 3-12 (object 212). Table 3-4 lists the layer thicknesses for the SDM Site model and the three alternatives for objects 207 and 212. The total thickness may differ because in order to avoid numerical instabilities a minimum layer thickness has to be assigned when transforming the geological layers into calculation layers. For the three alternatives, Alt1–Alt3, the minimum thickness was set to a very small number, only a few centimeters. The original SDM Site model had a minimum thickness of 1 m specified, which is the reason for the larger total thickness seen in object 212 in the SDM Site model.

The net precipitation is the precipitation minus all evapotranspiration components. Since MIKE SHE is driven by meteorological data, it is essential that the net precipitation is as correct as possible. If not, the model calibration will not give a physically correct description of the system. Therefore, the water balance results are mainly discussed from a precipitation point of view.

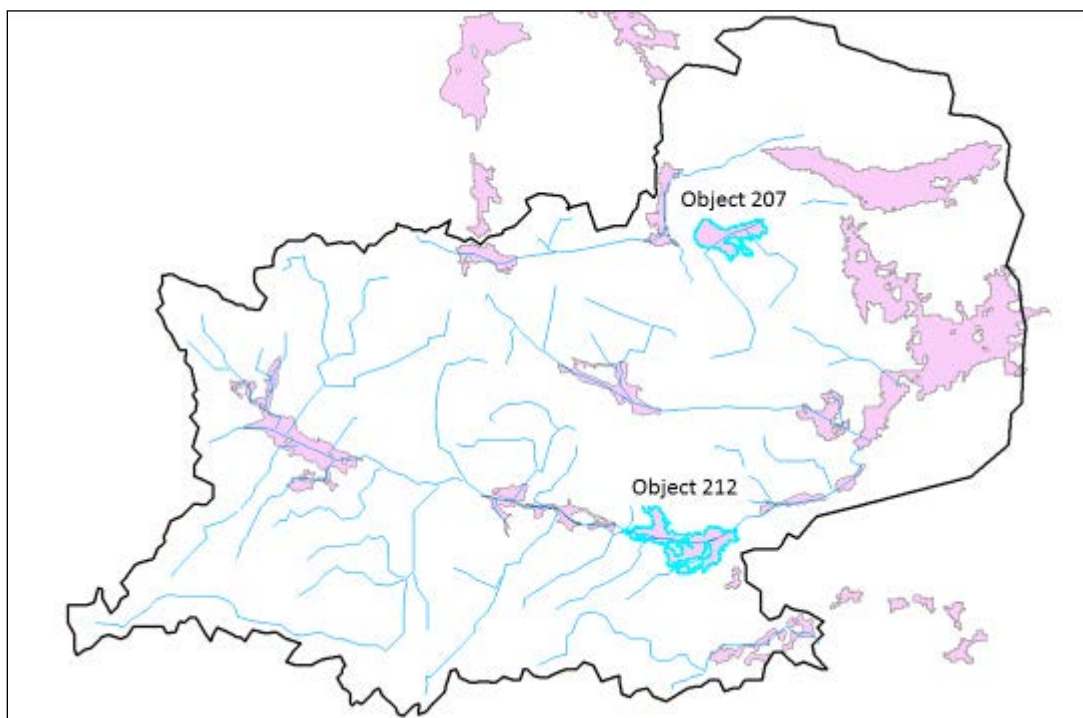


**Figure 3-10.** Location of the two objects in the regional model for which water balances according to Alt1–Alt3 as discussed in Chapter 2 were extracted.

### Object 207\_1 (Frisksjön)

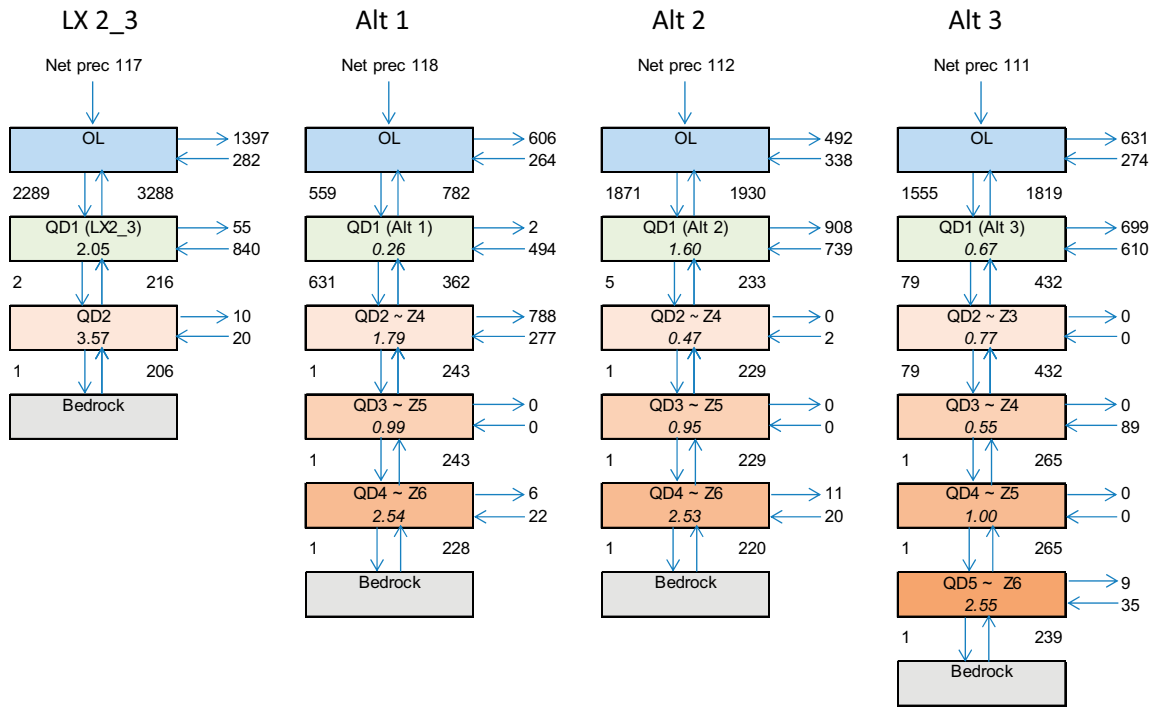


**Figure 3-11.** Water balances for Object 207 (Lake Frisksjön). Arrows represents net precipitation (Net prec) and surface and ground water flux rates (mm year<sup>-1</sup>). The average depth is listed within the box for each calculation layer (m) and in Table 3-4.

### Object 212\_2

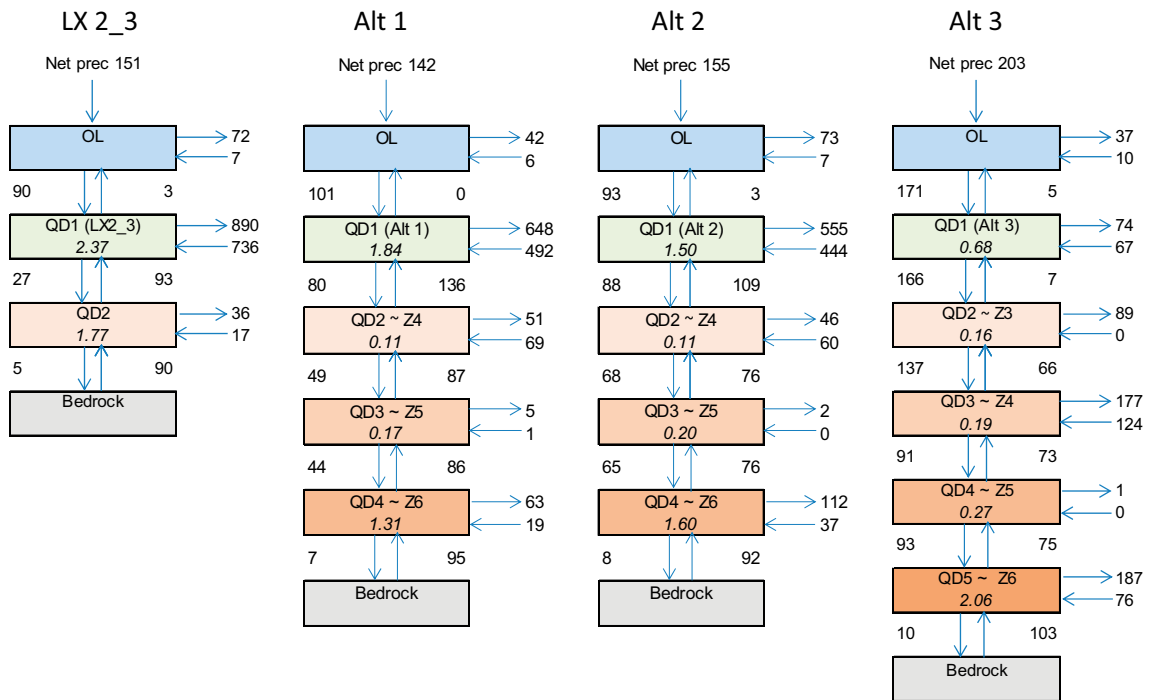


**Figure 3-12.** Water balances for object 212. Arrows represents net precipitation (Net prec) and surface and ground water flux rates (mm year<sup>-1</sup>). The average depth is listed within the box for each calculation layer (m), as well as in Table 3-4.

Figure 3-11 show that for object 207, which is Lake Frisksjön, the difference in net precipitation is small for all alternatives. This implies that the uppermost calculation layer is thick enough to allow for all surface processes to be fully active. As seen in Table 3-4, the uppermost layer for Alt1 is only 0.26 m and for Alt3 0.68 m. Since object 207 is a lake, thicknesses in that range is enough because the groundwater table is always above or very close to ground surface. For object 212 on the other hand, the difference in net precipitation is significantly larger, Figure 3-12. Alt3 has a net precipitation that is approximately 34 % larger than for the SDM Site model. Alt1 and Alt2 have more or less the same net precipitation as the SDM Site model. The larger net precipitation for Alt3 implies that the uppermost calculation layer isn't thick enough for this object, although it has the same thickness as for object 207. The groundwater level in object 212 is lower and more fluctuating than in object 207 and thus the evapotranspiration will be underestimated. Alt3 also has larger net flow from the bedrock to the regolith; this is partly an effect of the higher net precipitation yielding too much water in the model. The results for Alt1 and Alt2 are both comparable with the SDM Site results for object 212 as well as for object 207.

Looking beyond the precipitation, the main difference between the alternative models is that with more layers, and especially with layers following the geological layers, the horizontal flows are clearly occurring in the more permeable layers.

**Table 3-4. Thicknesses (m) of calculation layers in the regional model for objects 207 and 212.**

Object	Average layer thickness					Sum
	QD1	QD2	QD3	QD4	QD5	
<b>207</b>						
SDM-Site model	2.05	3.57				5.62
SFL Alt1	0.26	1.79	0.99	2.54		5.58
SFL Alt2	1.60	0.47	0.95	2.53		5.55
SFL Alt3	0.67	0.77	0.55	1.00	2.55	5.54
<b>212</b>						
SDM-Site model	2.37	1.77				4.14
SFL Alt1	1.84	0.11	0.17	1.31		3.43
SFL Alt2	1.50	0.11	0.20	1.60		3.41
SFL Alt3	0.68	0.16	0.19	0.27	2.06	3.36

All of the three alternative descriptions of calculation layers were set up with the purpose of having calculation layers as similar to the geological layers as possible but still have all the surface processes fully active. From the results discussed above it was concluded that Alt3 doesn't give satisfactory results.

For the local model, see Figure 2-5, the calculation layers were set according to Alt2. Figure 3-13 illustrates a profile through object 206 showing the calculation layers. The uppermost calculation layer, L1, consist of the geological layers Z1, Z2 and Z3 where the sum of the layers has a thickness of at least 1 m. The calculation layers L2, L3 and L4 follow the geological layers. The layers L5 and L6 are bedrock layers representing the surface bedrock which is more permeable and fractured than the deeper bedrock. The average thicknesses for the calculation layers in the regolith in object 206 are presented in Table 3-5.

All water balances extracted previously were based on values for an entire biosphere object. However, in many cases the transport through an object is taking place only in parts of the object. Furthermore, the size of the area with an active transport is depending on the soil properties. From a radionuclide modelling perspective, it would be preferable to describe the flows of groundwater through the different layers along the main path way for solute transport from the bedrock.

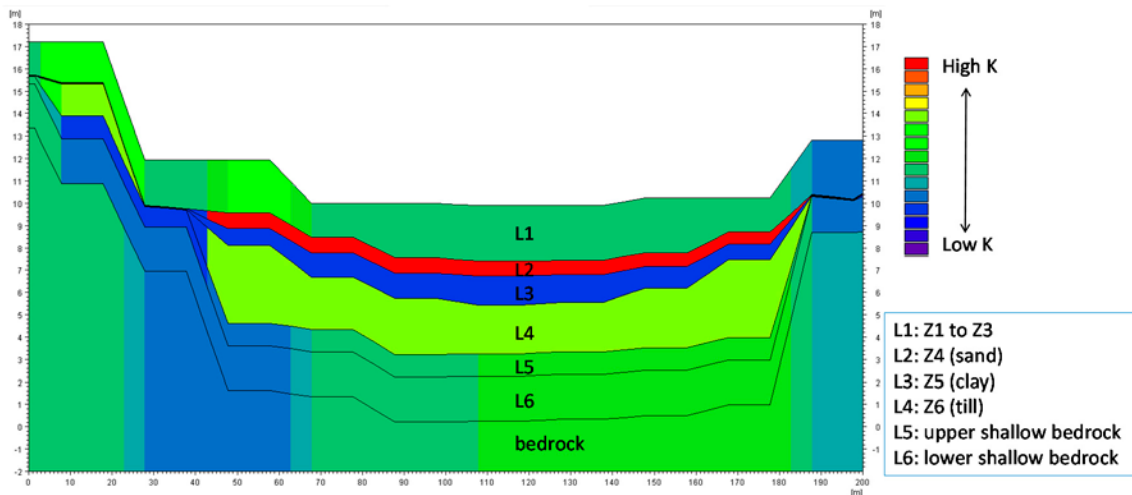


**Figure 3-13.** A profile through object 206 in the local model, showing the calculation layers

Figure 3-14 illustrates the area for the water balance based on the flow paths from the bedrock through the object. As discussed in Section 3.2, particle tracking starting positions were obtained from the ConnectFlow model (Joyce et al. 2019) and then further traced by particle tracking simulations in MIKE SHE. In Figure 3-14, the black line shows the extent of object 206. The dark cells (brown) are showing the starting positions for the particle tracking in MIKE SHE, i.e. they correspond to exit points from the bedrock in the ConnectFlow calculations (Joyce et al. 2019). As mentioned in Section 3.2, 500 particles were introduced in each of the brown cells in Figure 3-14. As the particles move towards the surface, they either concentrate or disperse. In MIKE SHE, the extraction of water balances is made for a certain area all over the depth of the model, and interpretations of results are difficult if mixing different areas for different layers. In order to find the most representative water balance area for the particle path lines, the area with starting points was extended for each layer by selecting all cells which had been hit by at least 500 particles. The cells added to the initial starting cells are marked in red in Figure 3-14. Thus the water balance area selected is the area with both red and brown cells. In total, the number of cells used for the water balance extraction was 259, which is twice as large as the area covered by the original starting positions in the bedrock (105), but still covers an area that is less than a third of the surface area of object 206 (which corresponds to 784 cells).

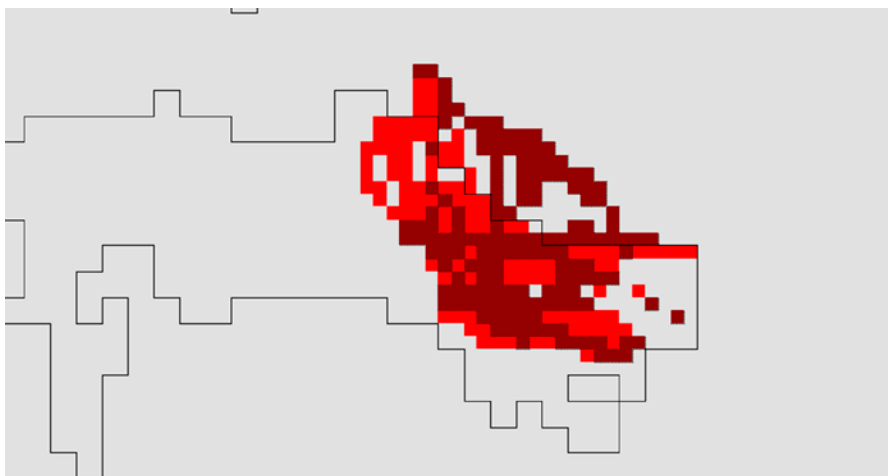


**Figure 3-14.** Water balance area for water balance presented in Figure 3-15. Brown cells represent the position of the discharge from the bedrock (PT2 in Figure 2-5). Red cells represent additional locations of the major flow paths that are not positioned right above a discharge point from the bedrock. Colored cells are used for the water balance extraction. Black solid line is showing the outer boundaries of object 206. Each grid cell represents an area of  $40 \times 40$  m.

**Table 3-5. Thicknesses of calculation layers in the local model for object 206**

Object	Average layer thickness				Sum
	L1	L2	L3	L4	
Entire object 206	2.28	0.49	0.93	2.84	6.54
Water balance area 206	2.23	0.43	0.78	2.15	5.59

Figure 3-15 shows the resulting water balance from MIKE SHE for the path dependent area selected according to Figure 3-14. The net annual precipitation is about 150 mm, which is in accordance with results based on the regional model. Since most of the introduced particles in the ConnectFlow model ends up within this object it is clear that it is a strong discharge area, and the net annual flux from the bedrock is about 215 mm. Object 206 is located above a large bedrock fracture, and a water balance for the entire object 206, show that the net annual flux from the bedrock is even higher, about 265 mm/year. However, although the entire object is a strong discharge area, the particles are concentrated to parts of the object, see Figure 2-5, due to the local topography and regolith thicknesses. Comparing this with the water balances extracted from the regional MIKE SHE model for objects 207 and 212 shows that it is in the same order as for object 207, which is Lake Frisksjön. The discharge to object 212 is significantly smaller, about 50 %.

Figure 3-15 also illustrate how the permeable sand layer, L2, has a large horizontal component with a net inflow of about 120 mm. Also the till has a net horizontal inflow, about 100 m, while there is no horizontal inflow at all in the clay layer. The thicknesses of the computational layers within the water balance area are presented in Table 3-5.

Based on the information from the particle tracking results, an estimation of how many cells in each layer are contributing to the main flow was made. Table 3-6 shows the number of “active” cells in each layer. An active cell is a cell which is hit by 500 particles or more. In L6, the number of active cells is 151, which is the number of cells with particles introduced within object 206, based on the ConnectFlow results. Moving through the shallow bedrock, the number of active cells are decreased somewhat but then increased again in the till. Above the till is clay, and here the number of active cells is only 1/3 of the initial number. In the sand layer, the particles are spread over a larger area again, and the number of active cells is greater than the initial. Finally, in the top layer, the number of active cells is about 50 % of the initial number.

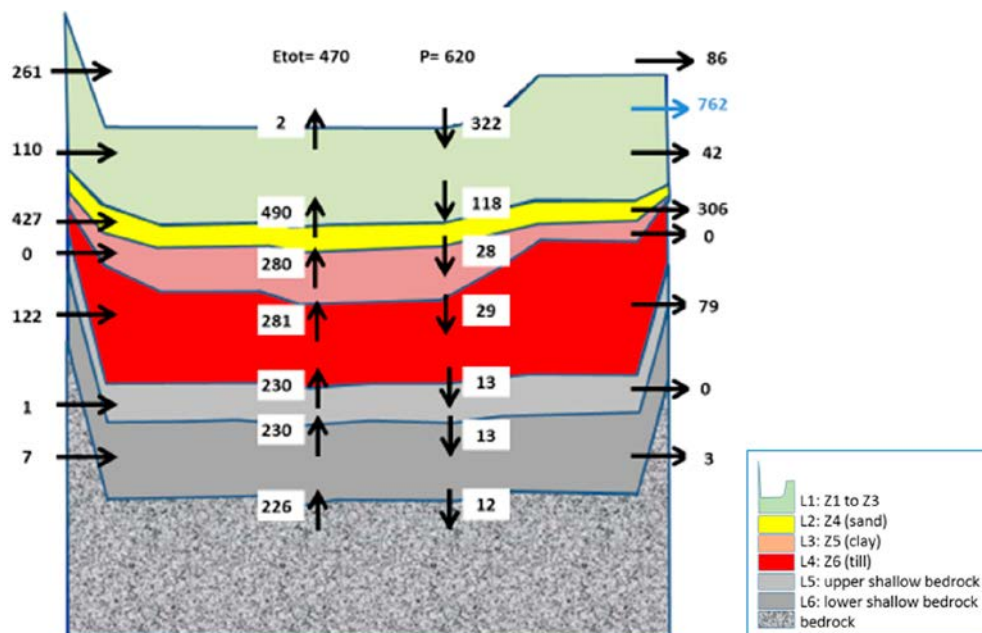


**Figure 3-15.** Water balance results for object 206, for the area illustrated in Figure 3-14. Blue color represents discharge to the central stream in the object. The area of the water balance corresponds to 259 cells. Units in mm per year. The average layer thicknesses are given in Table 3-5.

**Table 3-6. Number of active cells in each calculation layer.**

Layer	No of active cells	Active cells in % of starting cells
L1	76	50
L2	169	112
L3	50	33
L4	161	107
L5	115	76
L6	151	100

A way of graphically illustrating the active cells in the water balance figure is to scale the width of each layer with the number of active cells. Figure 3-16 illustrates how this would look for the active area of object 206. The width of the bedrock layer corresponds to the number of cells included in the water balance, which is 259. The width for layers above the bedrock is then scaled for the numbers given in Table 3-6. The average thicknesses are found in Table 3-5; no scaling with regard to depth is made in Figure 3-15.

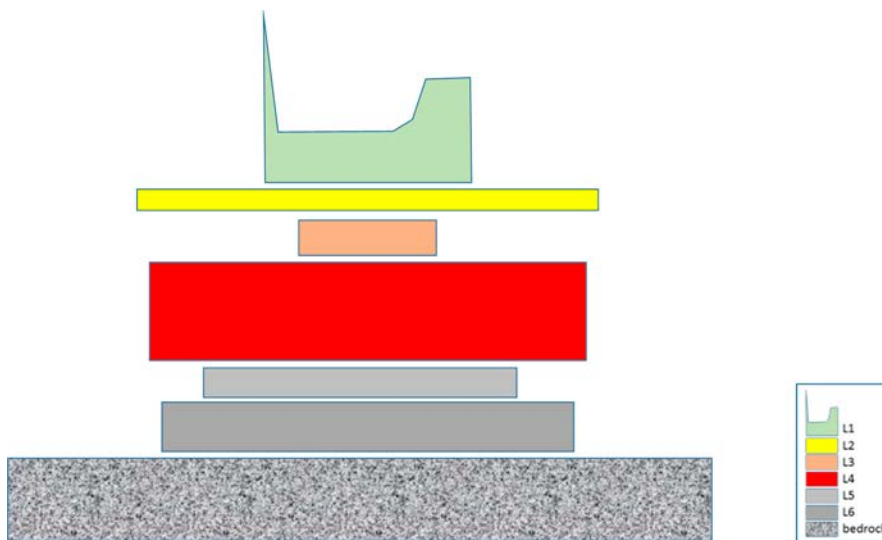


**Figure 3-16.** Translating the flow path within the area used for the water balance (Figure 3-15) into active cells for each calculation layer. The horizontal scale is proportional to the number of active cell. The layer thicknesses are given in Table 3-5; the figure is not scaled with regard to thicknesses.

## 4 Summary and discussion

### ***Discussion of numerical implementation of geological layers***

In MIKE SHE, the unsaturated zone (UZ) and evapotranspiration (ET) processes are fully described only in the uppermost numerical layer. Thus, to get a reasonable representation of the shallow groundwater dynamics the part of the soil profile where UZ and ET processes operates has to be included in the uppermost numerical layer. This constraint is in conflict with the desire to describe the groundwater flux (and transport) through each geological layer by defining calculation layers that are identical with the geological layers. However, the aim is to get as good representation of the geological stratigraphy as possible when defining the numerical layers.

In this study a sensitivity analysis was carried out aiming at identifying the optimal discretisation of numerical layers, taking the geology, UZ and ET processes into account. Three different alternatives for the numerical vertical discretization were implemented. In the first alternative, the upper calculation layer was described with focus on a lower level just below the average groundwater table. In the second alternative, the geological layers above the sand layer were lumped together although with a minimum thickness of 1 m. In the third option, only the peat and the surface layer were lumped together. For all alternatives, the numerical layers below the uppermost follow the geological layers.

Results indicate that the third alternative does not give satisfactory results in terms of evapotranspiration. The total annual evapotranspiration is about 90 % of the evapotranspiration in the other two alternatives and also in the SDM Site model. That means that there will be too much water in the model and the flows will be overestimated compared to measurements; this was also noted in the results for the surface stream discharges.

For the groundwater observation points, results in individual observation points differ between the three alternatives and the SDM Site model. The total average MAE values indicate that MAE values are comparable between all alternatives. No alternative have a higher total average MAE than the SDM Site model. The lowest average MAE is obtained for Alt2. The total average ME for Alt1 and Alt2 are both lower than for the SDM Site model. For Alt3, the total average ME is negative, while it is positive for the other alternatives and for the SDM Site model; this is an indication of that the higher net precipitation results in too high head elevations.

### ***Discussion of flow path dependent water balance and implications for dose models***

In previous water balance calculations for dose-modelling purposes the water balance of the whole biosphere object has been calculated. The biosphere object has been divided into mire and lake areas and the fluxes within and between the subareas has been calculated. Studying the particle flow path in detail, through the QD-layer from the bedrock/QD interface up to the different sinks at ground surface, it is seen that only a relatively small part of the biosphere object is exposed to groundwater discharge. Also, the flow paths are affected by the hydraulic properties in each layer. For example, due to the low hydraulic conductivity of glacial clay, particles are channelled to the areas with thinnest clay thickness along the way towards the surface. On the other hand, the high conductivity in the sand layers results in a predominantly horizontal flow path, which expose a relatively large area to released particles within the layer. The biosphere objects are often former lakes and the thickness of clay is therefore largest in the centre of the object (the deepest part of the lake). Accordingly, particles from the bedrock are primarily discharged into Quaternary deposits in locations close to the shoreline of the former lake. The different exposed areas along the particle flow paths might influence the concentration of radionuclides in the biosphere object. In this study we have presented an alternative way to calculate the fluxes of water between the QD-layers taking the flow paths and “exposed areas” in each QD-layer of the biosphere object into account. Using this approach the area exposed to radionuclides within each biosphere object is defined and dose calculations can be concentrated to these areas using the local properties and characteristics along the particle flow paths.

### ***Recommendations for future MIKE SHE applications***

The optimal coupling between geological and numerical layers is site specific and depends on the local hydrology and especially the general location of the groundwater table. The influence of UZ and ET processes on the dynamics of the groundwater table fluctuation is most sensitive in shallow groundwater systems. Based on results from this study it is concluded that an initial analysis of the QD layer and their spatial variation in relation to the groundwater table is recommended. For future modelling studies of the Forsmark site, where the groundwater table is shallow and ET processes having a strong influence on the groundwater dynamics, alternative 2 is probably the best option of the alternative tested in this study. Keeping the geological description in the numerical implementation of the model enables a more detailed flow path analysis through the QD layers such that the exposed area within each biosphere object can be identified and analysed in more detail.

## References

SKB's (Svensk Kärnbränslehantering AB) publications can be found at [www.skb.com/publications](http://www.skb.com/publications).

**Bear J, 1979.** *Hydraulics of groundwater*. New York: McGraw-Hill.

**Bosson E, Sassner M, Gustafsson L-G, 2009.** Numerical modelling of surface hydrology and near-surface hydrogeology at Laxemar-Simpevarp. Site descriptive modelling, SDM-Site Laxemar. SKB R-08-72, Svensk Kärnbränslehantering AB.

**Bosson E, Sassner, Sabel U, Gustafsson L-G, 2010.** Modelling of present and future hydrology and solute transport at Forsmark. SR-Site Biosphere. SKB R-10-02, Svensk Kärnbränslehantering AB.

**Elfving M, Evins L Z, Gontier M, Graham P, Mårtensson P, Thunbrant S, 2013.** SFL concept study. Main report. SKB TR-13-14, Svensk Kärnbränslehantering AB.

**Graham D N, Butts M B, 2005.** Flexible integrated watershed modeling with MIKE SHE. In Singh V P, Frevert D K (eds). *Watershed models*. CRC Press, 245–272.

**Joyce S, Appleyard P, Hartley L, Tsitsopoulos V, Woollard H, Marsic N, Sidborn M, Crawford J, 2019.** Groundwater flow and reactive transport modelling of temperate conditions. Report for the safety evaluation SE-SFL. SKB R-19-02, Svensk Kärnbränslehantering AB.

**Klos R, Wörman A, 2015.** Supplementary review of SKB's further RFI response. Main review phase. Technical Note 2015:48, Swedish Radiation Safety Authority.

**Morris D A, Johnson A I, 1967.** Summary of hydrologic and physical properties of rock and soil materials, as analyzed by the hydrologic laboratory of the U.S. Geological Survey, 1948–60. Water Supply Paper 1839-D, U. S. Government Printing Office, Washington.

**Nyman H, Sohlenius G, Strömgren M, Brydsten L, 2008.** Depth and stratigraphy of regolith. Site descriptive modelling, SDM-Site Laxemar. SKB R-08-06, Svensk Kärnbränslehantering AB.

**Rhén I, Forsmark T, Hartley L, Joyce S, Roberts D, Gylling B, Marsic N, 2009.** Bedrock hydrogeology. Model testing and synthesis. Site descriptive modelling, SDM-Site Laxemar. SKB R-08-91, Svensk Kärnbränslehantering AB.

**Sohlenius G, Hedenström A, 2008.** Description of regolith at Laxemar-Simpevarp. Site descriptive modelling SDM-Site Laxemar. SKB R-08-05, Svensk Kärnbränslehantering AB.

**SSM, 2018.** Strålsäkerhet efter slutförvarets förslutning. Beredning inför regeringens prövning Slutförvaring av använt kärnbränsle. Rapport 2018:07, Swedish Radiation Safety Authority. (In Swedish.)

**Strömgren M, Brydsten L, Lindgren F, 2006.** Oskarshamn site investigation. Measurements of brook gradients. SKB P-06-05, Svensk Kärnbränslehantering

**Söderbäck B, Lindborg T, 2009.** Surface system Laxemar-Simpevarp. Site descriptive modelling SDM-Site Laxemar. SKB R-09-01, Svensk Kärnbränslehantering AB.

**Werner K, 2009.** Description of surface hydrology and near-surface hydrogeology at Laxemar-Simpevarp. Site descriptive modelling, SDM-Site Laxemar. SKB R-08-71, Svensk Kärnbränslehantering AB.

**Werner K, Öhman J, Holgersson B, Rönnback K, Marelius F, 2008.** Meteorological, hydrological and hydrogeological monitoring data and near-surface hydrogeological properties data from Laxemar-Simpevarp. Site descriptive modelling, SDM-Site Laxemar. SKB R-08-73, Svensk Kärnbränslehantering AB.

**Werner K, Sassner M, Johansson E, 2013.** Hydrology and near-surface hydrogeology at Forsmark – synthesis for the SR-PSU project. SR-PSU biosphere. SKB R-13-19, Svensk Kärnbränslehantering AB.



## Tables with MAE and ME values

Table A-1. MAE and ME values for SSM observation points, evaluated as head elevations.

	MAE for head elevation							
	SDM Site model		SFL Alt1		SFL Alt2		SFL Alt3	
	MAE	ME	MAE	ME	MAE	ME	MAE	ME
SSM000011	0.66	-0.58	0.89	0.79	0.90	0.80	0.88	0.77
SSM000017	0.70	0.66	0.49	0.47	0.25	-0.25	0.33	-0.33
SSM000019	0.34	0.09	0.29	-0.14	0.31	0.02	0.94	-0.94
SSM000021	0.22	-0.18	0.28	-0.27	0.23	-0.19	0.40	-0.39
SSM000030	0.10	0.00	0.29	-0.29	0.26	-0.26	0.65	-0.65
SSM000031	0.27	0.27	0.18	0.18	0.20	0.20	0.18	-0.05
SSM000032	0.33	-0.33	0.54	-0.54	0.34	-0.34	0.56	-0.56
SSM000033	0.65	0.37	0.34	-0.24	0.51	0.13	1.38	-1.38
SSM000034	0.47	-0.45	0.91	-0.91	0.74	-0.74	1.09	-1.09
SSM000037	0.72	-0.72	0.97	-0.97	1.12	-1.12	1.37	-1.37
SSM000039	0.37	-0.19	0.44	-0.40	0.41	-0.35	0.69	-0.63
SSM000041	0.37	-0.37	0.48	-0.48	0.44	-0.44	0.70	-0.70
SSM000042	0.29	0.28	0.14	0.11	0.23	0.21	0.14	-0.08
SSM000210	0.49	-0.18	0.43	-0.23	0.75	0.72	0.37	0.24
SSM000213	1.16	1.16	1.01	1.01	1.00	1.00	0.68	0.68
SSM000219	1.36	1.36	1.14	1.14	0.97	0.89	0.56	0.29
SSM000220	0.85	0.77	0.68	0.64	0.44	0.40	0.58	-0.36
SSM000221	0.88	0.81	0.70	0.60	0.40	0.29	0.37	-0.05
SSM000222	0.14	-0.03	0.29	-0.28	0.43	-0.43	0.69	-0.69
SSM000223	0.14	-0.04	0.24	-0.22	0.39	-0.37	0.60	-0.60
SSM000224	0.21	0.19	0.31	0.31	0.31	0.31	0.28	0.28
SSM000225	0.22	0.20	0.33	0.33	0.32	0.32	0.29	0.29
SSM000226	0.83	0.74	0.64	0.56	2.03	-2.03	0.86	-0.86
SSM000227	0.53	0.44	0.54	0.37	0.56	-0.06	0.55	-0.14
SSM000228	0.22	0.18	0.14	0.09	0.17	0.12	0.23	-0.20
SSM000229	0.84	0.79	0.90	0.88	0.88	0.87	0.59	0.23
SSM000230	1.08	-1.08	1.38	-1.38	1.52	-1.52	1.61	-1.61
SSM000237	0.98	0.98	0.86	0.81	0.94	0.93	0.27	-0.05
SSM000239	0.14	-0.14	0.27	-0.27	0.28	-0.28	0.34	-0.34
SSM000240	0.04	0.02	0.09	-0.09	0.08	-0.08	0.11	-0.11
SSM000242	0.43	-0.43	0.87	-0.87	0.86	-0.86	1.11	-1.11
SSM000249	0.73	-0.64	1.05	0.12	0.70	-0.68	0.65	-0.26
SSM000250	1.50	1.50	1.04	0.91	1.01	0.88	0.70	-0.51
	<b>0.55</b>	<b>0.17</b>	<b>0.58</b>	<b>0.05</b>	<b>0.61</b>	<b>-0.06</b>	<b>0.63</b>	<b>-0.37</b>

**Table A-2. MAE and ME values for SSM observation points, evaluated as depth to phreatic surface.**

	MAE for depth to phreatic surface							
	SDM Site model		SFL Alt1		SFL Alt2		SFL Alt3	
	MAE	ME	MAE	ME	MAE	ME	MAE	ME
SSM000011	0.76	-0.53	0.90	-0.82	0.96	-0.81	1.76	-1.75
SSM000017	1.33	-1.33	1.47	-1.47	0.27	0.11	0.29	-0.29
SSM000019	0.34	0.09	0.29	-0.14	0.31	0.02	0.93	-0.93
SSM000021	1.13	-1.13	1.26	-1.26	0.16	0.10	0.17	-0.09
SSM000030	0.53	0.53	0.43	0.43	0.49	0.49	0.21	0.18
SSM000031	0.74	-0.74	0.78	-0.78	0.78	-0.78	0.82	-0.82
SSM000032	0.19	-0.16	0.40	-0.40	0.18	-0.13	0.40	-0.40
SSM000033	0.66	0.38	0.36	-0.27	0.51	0.13	1.42	-1.42
SSM000034	0.34	-0.28	0.46	-0.46	0.35	-0.27	0.62	-0.62
SSM000037	0.47	-0.47	0.53	-0.53	0.52	-0.52	0.56	-0.56
SSM000039	0.30	-0.10	0.56	-0.54	0.50	-0.46	0.72	-0.70
SSM000041	1.97	1.97	1.87	1.87	1.84	1.84	1.67	1.67
SSM000042	0.30	0.29	0.15	0.11	0.23	0.22	0.14	-0.07
SSM000210	1.33	-1.32	1.35	-1.35	0.75	0.70	0.52	-0.23
SSM000213	1.27	1.27	1.10	1.10	1.03	1.03	0.68	0.68
SSM000219	1.26	1.25	0.88	0.85	0.85	0.32	0.61	-0.24
SSM000220	2.13	2.13	1.40	1.40	1.15	1.15	0.85	0.79
SSM000221	1.12	1.12	0.92	0.91	0.63	0.62	0.34	0.25
SSM000222	0.21	0.17	0.17	0.11	0.18	0.13	0.16	0.09
SSM000223	0.52	-0.52	0.58	-0.58	0.78	-0.78	0.80	-0.80
SSM000224	0.63	0.63	0.73	0.73	0.73	0.73	0.69	0.69
SSM000225	0.64	0.64	0.74	0.74	0.74	0.74	0.70	0.70
SSM000226	2.81	-2.81	3.09	-3.09	1.22	-1.21	1.50	-1.50
SSM000227	1.63	-1.63	1.76	-1.76	1.41	-1.41	2.01	-2.01
SSM000228	0.21	0.18	0.14	0.10	0.18	0.14	0.25	-0.22
SSM000229	1.19	1.19	0.63	0.59	0.63	0.59	0.50	-0.15
SSM000230	0.84	-0.84	1.14	-1.14	1.28	-1.28	1.37	-1.37
SSM000237	0.96	0.96	0.77	0.70	0.83	0.82	0.31	-0.22
SSM000239	0.03	-0.03	0.03	-0.03	0.03	-0.03	0.03	-0.03
SSM000240	0.05	0.03	0.04	0.03	0.04	0.03	0.05	0.03
SSM000242	1.92	1.92	2.01	2.01	0.14	0.12	0.12	0.04
SSM000249	0.73	-0.65	2.30	1.31	0.70	-0.68	1.33	0.42
SSM000250	1.81	1.73	1.43	1.30	1.38	1.25	0.72	-0.50
	<b>0.92</b>	<b>0.12</b>	<b>0.93</b>	<b>-0.01</b>	<b>0.66</b>	<b>0.09</b>	<b>0.71</b>	<b>-0.28</b>

**Table A-3. MAE and ME values for bedrock observation points, evaluated as head elevations.**

	MAE for head elevation							
	SDM Site model		SFL Alt1		SFL Alt2		SFL Alt3	
	MAE	ME	MAE	ME	MAE	ME	MAE	ME
HLX01_1b	0.44	-0.23	0.45	-0.23	0.44	-0.21	0.78	-0.73
HLX02_1	2.66	2.66	2.44	2.44	2.61	2.61	2.13	2.13
HLX06_1	1.07	0.83	1.16	0.98	1.27	1.17	0.86	0.49
HLX07_1	0.56	-0.05	0.56	0.03	0.58	0.19	0.60	-0.27
HLX08_1	0.63	-0.63	0.63	-0.63	0.65	-0.65	0.79	-0.79
HLX09_1b	1.03	-1.03	1.11	-1.11	1.13	-1.13	1.24	-1.24
HLX09_2b	0.33	0.02	0.35	-0.03	0.36	-0.06	0.34	-0.16
HLX11_1	0.38	-0.06	0.35	-0.15	0.36	-0.14	0.67	-0.63
HLX11_2	0.39	-0.13	0.38	-0.22	0.38	-0.21	0.74	-0.71
HLX13_1	1.17	1.17	1.04	1.04	0.97	0.97	0.62	0.60
HLX14_1	0.79	0.79	0.65	0.64	0.59	0.56	0.44	0.21
HLX15_1	0.65	0.65	0.44	0.42	0.35	0.28	0.35	-0.16
HLX18_1	0.67	-0.67	0.88	-0.88	0.92	-0.92	1.34	-1.34
HLX18_2	0.41	-0.41	0.61	-0.60	0.64	-0.64	0.92	-0.92
HLX21_1c	0.38	0.26	0.32	0.15	0.30	0.07	0.45	-0.36
HLX21_2b	0.35	0.26	0.30	0.19	0.29	0.11	0.39	-0.21
HLX22_1b	0.69	0.65	0.58	0.51	0.52	0.45	0.33	-0.01
HLX22_2	1.10	-1.09	1.17	-1.16	1.25	-1.24	1.56	-1.56
HLX23_1	0.83	0.81	0.71	0.68	0.68	0.64	0.37	0.10
HLX23_2	0.45	0.25	0.37	0.13	0.35	0.10	0.39	-0.29
HLX24_1c	0.72	0.66	0.61	0.54	0.59	0.51	0.36	0.04
HLX24_2b	0.74	0.74	0.62	0.62	0.59	0.59	0.34	0.16
HLX25_1b	0.52	0.08	0.48	-0.02	0.50	-0.10	0.66	-0.55
HLX25_2b	0.49	-0.11	0.44	-0.11	0.47	-0.21	0.65	-0.60
HLX26_1	1.08	-1.08	1.29	-1.29	1.44	-1.44	1.84	-1.84
HLX27_1b	0.46	-0.43	0.60	-0.59	0.69	-0.68	1.14	-1.14
HLX27_2	0.52	-0.51	0.67	-0.66	0.77	-0.77	1.26	-1.26
HLX28_1	3.45	3.45	3.46	3.46	3.34	3.34	2.93	2.93
HLX30_1b	0.42	-0.18	0.42	-0.28	0.44	-0.34	0.80	-0.80
HLX30_2b	0.38	-0.16	0.41	-0.32	0.44	-0.38	0.81	-0.80
HLX31_1a	0.40	-0.18	0.41	-0.26	0.42	-0.35	0.71	-0.71
HLX31_1b	0.47	0.23	0.42	0.10	0.40	0.07	0.48	-0.38
HLX31_2	0.37	0.36	0.28	0.26	0.23	0.21	0.21	-0.09
HLX33_1	0.62	0.58	0.51	0.45	0.47	0.39	0.30	-0.06
HLX33_2	0.43	0.39	0.32	0.26	0.28	0.21	0.24	-0.12
HLX34_1	1.80	1.80	1.61	1.61	1.49	1.49	1.06	1.03
HLX35_1	1.43	1.21	1.37	1.10	1.28	0.96	1.02	0.54
HLX35_2	0.56	-0.44	0.58	-0.54	0.72	-0.69	1.04	-1.04
HLX36_1a	0.38	0.20	0.35	0.15	0.36	0.06	0.43	-0.30
HLX36_1b	3.01	3.01	2.93	2.93	2.85	2.85	2.31	2.31
HLX36_2	0.24	-0.13	0.24	-0.17	0.28	-0.24	0.66	-0.66
HLX38_1	1.49	-1.49	1.62	-1.62	1.75	-1.75	2.29	-2.29
HLX39_1	1.97	1.97	2.08	2.08	1.93	1.93	1.33	1.33
HLX40_1	2.75	2.75	2.63	2.63	2.48	2.48	1.88	1.88
HLX41_1	3.35	3.35	3.28	3.28	3.11	3.11	2.53	2.53
HLX43_1	1.88	1.88	1.73	1.73	1.59	1.59	0.80	0.80
HLX43_2	3.97	3.97	3.10	3.10	3.10	3.10	2.76	2.76
HLX21_1e	0.44	0.33	0.36	0.17	0.36	0.14	0.47	-0.42
HLX21_2c	0.40	0.31	0.31	0.16	0.31	0.15	0.36	-0.30
HLX32_1	2.82	-2.82	2.93	-2.93	3.04	-3.04	3.55	-3.55
	<b>1.05</b>	<b>0.48</b>	<b>1.01</b>	<b>0.36</b>	<b>1.01</b>	<b>0.30</b>	<b>1.01</b>	<b>-0.13</b>

SKB is responsible for managing spent nuclear fuel and radioactive waste produced by the Swedish nuclear power plants such that man and the environment are protected in the near and distant future.

**skb.se**